

Proposal of new distribution coefficients (K_d) of potentially toxic elements in soils for improving environmental risk assessment in the State of São Paulo, southeastern Brazil

Marcio Roberto Soares ^{a,*}, Jorge Eduardo de Souza Sarkis ^b, Luís Reynaldo Ferracciú Alleoni ^c

^a Department of Natural Resources and Environmental Protection, Agrarian Sciences Center, Federal University of São Carlos, Rodovia Anhanguera, km 174, 13600-970, P.O. Box 173, Araras, SP, Brazil

^b Lasers and Applications Center, Nuclear and Energy Research Institute, Avenida Lineu Prestes n° 2242, 05508-000, São Paulo, SP, Brazil

^c Department of Soil Science, Luiz de Queiroz College of Agriculture, University of São Paulo, Avenida Pádua Dias n° 11, 12418-900, Piracicaba, SP, Brazil

ARTICLE INFO

Keywords:

Tropical soils
Soil contamination
Regulatory guiding values
Risk assessment
Environmental public policy

ABSTRACT

Soil solid-solution distribution coefficients (K_d) are used in predictive environmental models to assess public health risks. This study was undertaken to determine K_d for potentially toxic elements (PTE) Cd, Co, Cr, Cu, Ni, Pb, and Zn in topsoil samples (0–20 cm) from 30 soils in the State of São Paulo, southeastern Brazil. Batch sorption experiments were carried out, and PTE concentrations in the equilibrium solution were determined by High Resolution Inductively Coupled Plasma Mass Spectrometry (HR-ICPMS). Sorption data was fitted to the Freundlich model. The K_d values were either obtained directly from the slope coefficients of C-type isotherms or derived from the slope of the straight line tangent to the non-linear L-type and H-type isotherms. Stepwise multiple regression models were used to estimate the K_d values through the combined effect of a number of soil attributes [pH_{H2O} , effective cation exchange capacity (ECEC) and contents of clay, organic carbon, and Fe (oxy) hydroxides]. The smallest variation in K_d values was recorded for Cu (105–4598 L kg⁻¹), Pb (121–7020 L kg⁻¹), Ni (6–998 L kg⁻¹), as variation across four orders of magnitude was observed for Cd (7–14,339 L kg⁻¹), Co (2–34,473 L kg⁻¹), and Cr (1–21,267 L kg⁻¹). The K_d values for Zn were between 5 and 123,849 L kg⁻¹. According to median values of K_d , PTE were sorbed in the following preferential order: Pb > Cu > Cd > Ni > Zn > Cr > Co. The K_d values were best predicted using metal-specific and highly significant ($p < 0.001$) linear regressions that included pH_{H2O} , ECEC, and clay contents. The K_d values reported in this study are a novel result that can help minimize erroneous estimates and improve both environmental and public health risk assessments under humid tropical edaphoclimatic conditions.

1. Introduction

The State of São Paulo has the largest population of all Brazilian states, estimated at 45 million inhabitants living in 645 municipalities (248,219 km²). In Brazil it is the most important area in terms of economic power (accounting for 35% of Brazil's Gross National Product) and diversity of agricultural, industrial, and agroindustrial activities (sugar-alcohol, textile, metal-mechanical, chemical, automotive, aeronautic, and computer industries, as well as the service and financial sectors) (IBGE, 2019) logically accessible with the most extensive statewide road transportation system in Brazil (34,650 km).

Hazardous inorganic elements are a category of soil and groundwater contaminants that have never been precisely defined in the

scientific literature (Wuana and Okieimen, 2011). Inorganic elements listed as a high-priority issue for food security, human health, and environmental protection include (Jennings, 2013; USEPA, 2015a; CETESB, 2016; ATSDR, 2019; Rai et al., 2019): transition metals - Ag, Cd, Co, Cr, Cu, Fe, Hg, Mn, Mo, Ni, V, and Zn; post-transition metals - Al, Pb, and Tl; metalloids or semi-metals - As, B, and Sb; alkali earth metals - Ba and Be; and non-metals - Se.

Potentially toxic elements (PTE) have been considered a more inclusive and appropriate term (Shaheen et al., 2013) to refer to this broad set of essential and non-essential elements for plant and animal metabolism, with the potential for toxicity and a resulting threat to live organisms depending on their concentration (Abrahams, 2002). The PTE occur naturally as background concentrations in the soil environment from the weathering of geological parent material (Alloway, 2013).

* Corresponding author.

E-mail addresses: mrsoares@ufscar.br (M.R. Soares), jesarkis@ipen.br (J.E. de Souza Sarkis), alleoni@usp.br (L.R.F. Alleoni).

Abbreviations

K_d	solid-solution distribution coefficient
PTE	potentially toxic element
RGV	regulatory guiding value
QRV	quality reference value
PV	prevention value
IV	intervention value
CETESB	Environmental Company of the State of São Paulo, Brazil
HR-ICPMS	High Resolution Inductively Coupled Plasma Mass Spectrometry
CEC	cation exchange capacity
ECEC	effective cation exchange capacity
OC	organic carbon
SOC	soil organic carbon
DOC	dissolved organic carbon
OM	organic matter
SOM	soil organic matter
DOM	dissolved organic matter
Fe _{Na-DCB}	iron oxides extracted by sodium dithionite-citrate-bicarbonate
Fe _{Ox}	iron oxides extracted by ammonium acid oxalate

Several activities in modern society are anthropogenic sources of PTE inputs to soil, such as atmospheric deposition, mining activities, unregulated landfills, sewage sludge, livestock manure, inorganic fertilizers, agrochemicals, coal combustion residues, spillage of petrochemicals, automobile traffic (exhaust, burning leaded gasoline, and dust from tire wear), and indiscriminate industrial waste disposal practices (Alloway, 2013; Matusiewicz and Bulska, 2018; Canteras et al., 2019; Palansooriya et al., 2020).

There are over 20 million ha of land contaminated by PTE around the world (Liu et al., 2018). For the EU-28, an estimate of around 2.5–2.8 million sites where soil polluting activities took/are taking place was obtained. The main contaminant category was heavy metals contributing to around 35% and 31% of the soil and groundwater contamination, respectively (Panagos et al., 2013; Pérez and Eugenio, 2018). In the United States, it is estimated that 294,000 sites need to be cleaned (USEPA, 2014) and 1344 uncontrolled hazardous waste sites are placed on the Superfund's National Priorities List (USEPA, 2018).

Environmental authorities in Brazil have increasingly detected soil and groundwater contamination. Currently, the State of São Paulo has a soil policy enacted by the 2009 State Act n° 13,577 (SÃO PAULO, 2009; Spínola and Philippi Jr., 2011). The state government is responsible for environmental management through the Environmental Company of the State of São Paulo (CETESB), which conducts systematic technical studies to identify high-priority contaminated sites. Of the 6285 sites listed in the last survey, 1374 were declared directly contaminated by PTE (CETESB, 2019). State Act n° 13,577 also supported the drafting of the Resolution of the National Environment Council of Brazil No. 420 (CONAMA, 2009), a soil regulatory approach that resembles the Dutch policy and distinguishes three main levels of contamination (CONAMA, 2009; Spínola and Phillipi Jr., 2011; Swartjes et al., 2012; CETESB, 2016): (i) negligible risk or quality reference values (QRV) (natural or background PTE concentration of clean soil or natural quality of groundwater); (ii) intermediate risk or prevention values (PV) (warning PTE concentration above which it is necessary to monitor harmful changes to environmental quality); and (iii) potentially unacceptable risk or intervention values (IV) (threshold PTE concentration above which the site is contaminated and a gradual risk assessment is applied to intercede and treat the site).

Increasingly geological surveys of the extent of contamination on the

regional (Fabietti et al., 2009), national (Brus et al., 2009; Smith et al., 2013), or continental scales (Caritat et al., 2018) have been developed from which regulatory guiding values (RGV) have been established. The derivation methods of RGV in most environmental protection regulations have scientific and political bases and, as an important tool in the development of public policy, they characterize contaminated areas, restrict licenses, and define infractions, as well as the imposition of penalties (Swartjes et al., 2012; Jennings, 2013; Rodrigues et al., 2009).

Major international policies and guidelines pertaining to the control of soil and groundwater quality are based on the total or pseudototal PTE content often extracted by microwave assisted acid digestions (Sauvé et al., 2000). The *aqua regia* ISO 12914 method (1:3 HNO₃:HCl ratio) (ISO, 2012) has been used as the standard for soil certification in most European Union countries. The 3051A (HNO₃ or 3:1 HNO₃:HCl ratio) and 3052 (3:1 HNO₃:HF ratio) methods [USEPA SW 846 3000 series protocols; (USEPA, 2015c)] are also extensively used in the United States and internationally by environmental agencies.

The (pseudo)total content can be useful as a first approach to soil contamination through the establishment of background or QRV, but it is inappropriate for assessing either the ecological or human health risks since it does not represent accurate information about the bioavailable fractions of PTE (Houba et al., 1996). In soils, PTE from anthropogenic sources tend to be more mobile and bioavailable than pedogenic or lithogenic ones (Wuana and Okiemien, 2011) because PTE interact with soil components and thereby change the effect of their activity and mobility (Galán et al., 2019).

Equilibrium partitioning of PTE between soil phases controls their distribution, fate, mobility, and bioavailability and can be characterized by the solid-solution distribution coefficient (K_d) (Anderson and Christensen, 1988; Buchter et al., 1989; Sheppard and Thibault, 1990; Bockting et al., 1992; USEPA, 1999; Sauvé et al., 2000; Tipping et al., 2003; Environmental Agency, 2005; Allison and Allison, 2005; Degryse et al., 2009; Gil-García et al., 2009; Braz et al., 2013a; 2013b; Shaheen et al., 2013; Schneider et al., 2019). Distribution coefficient is a key parameter since the remediation of PTE contaminated soils is achieved through the manipulation of their bioavailability (Bolan et al., 2014). It provides an assessment of sorption properties for comparing different soils with respect to a given PTE under given conditions (Bockting et al., 1992; Shaheen et al., 2013).

Sorption is a broad term that refers to processes by which ions can bind to solid surfaces and through which soil is capable of retaining contaminants avoiding their passing to more sensitive media such as the hydrosphere and biosphere (Bradl, 2004; Galán et al., 2019). This process is recognized as an important natural or enhanced mechanism for attenuating soil contamination as an intrinsic remediation (Young and Mulligan, 2019). Therefore, K_d should be acquired from experimental protocols where the sorption process controls aqueous PTE concentrations and normally these conditions are fulfilled in so-called batch sorption experiments (USEPA, 2008; Soares and Casagrande, 2009).

Sorption data is commonly described as a thermodynamic equilibrium process and is modeled by sorption isotherms (Hinz, 2001; Limousin et al., 2007). Distribution coefficient is derived from the adjustment of experimental data to the Freundlich equation which mathematically describes a kind of sorption characterized by the C-type or constant partition isotherm (Fontes and Alleoni, 2006; Soares and Casagrande, 2009). Potentially toxic elements K_d is then calculated as $K_d = \text{PTE}_{\text{sorbed}}/\text{PTE}_{\text{solution}}$, where $\text{PTE}_{\text{sorbed}}$ is the chemical concentration sorbed to solid phase (mg kg^{-1}) and $\text{PTE}_{\text{solution}}$ is the chemical concentration in aqueous solution (mg L^{-1}), under equilibrium conditions.

Although somewhat simplistic, the constant K_d approach is frequently applied, because it is easily integrated into the main internationally renowned environmental forecasting and ecotoxicological risk models (Chang et al., 2001; Degryse et al., 2009), such as the CLEA in the United Kingdom, the RBCA Tool Kit in the United States, and the CSOIL in the Netherlands (Otte et al., 2001; Brand et al., 2007; Jeffries

and Martin, 2009; Yen Le and Hendricks, 2014; Lee et al., 2019).

The efficacy of risk assessment depends on the reliability of parameter values employed in the computations (Chen et al., 2009). Important factors, such as bioavailability, biotransference, and leaching should be calculated instead of using the values preset by the program (Galán et al., 2019). Obtaining or selecting K_d is a critical step that precedes the calculation of factors included in the main risk forecasting models, such as the bioconcentration factor (BCF) (Otte et al., 2001), soil-to-root concentration and plant uptake factors (USEPA, 1996; Chen et al., 2009; Jeffries and Martin, 2009), chemical retardation factor (Rf) (Chang et al., 2001; Degryse et al., 2009), soil-water partition coefficient normalized to organic carbon (K_{OC}) (Vitale and Di Guardo, 2019), and the maximum permissible concentration (MPC) for the derivation of quality standards for soil and groundwater (Crommentuijn et al., 1997).

Distribution coefficients for inorganic chemicals can be based on measured values derived from geochemical data or on estimation methods. The procedure for the management of contaminated areas in the State of São Paulo established the application of its own worksheets to human health risk analysis in contaminated areas subjected to investigation (CETESB, 2017). As with many other models, CETESB estimates IV for soils and groundwater based on the fraction of the PTE present in the soil solution. Since the main PTE exposure routes to derive IV are drinking water and vegetable consumption, K_d plays a pivotal role as a bioavailability descriptor (Otte et al., 2001; Augustsson et al., 2016).

Due to the restricted availability, generic values of K_d selected from the scientific literature, mainly data from temperate regions (e.g. United States, Netherlands, or United Kingdom databases), have often been used as the default parameter of PTE bioavailability. CETESB's current spreadsheets (CETESB, 2020) incorporate scientific knowledge about toxicological and physicochemical parameters (including K_d) of the Risk Screening Levels (RSLs) of USEPA's "Superfund" program (USEPA, 2019) and USEPA's Integrated Risk Information System (IRIS) (USEPA, 2020). The calculation of RGV is based on the procedure described in the Risk Assessment Guidance for Superfund (USEPA RAGS) (USEPA, 1989) using default values in standardized equations. It is doubtful, therefore, whether the current environmental assessment models, based datasets of temperate regions, will be valid for tropical settings (Rieuwerts, 2007).

Default values from different edaphoclimatic zones can lead to results that may differ by several orders of magnitude and to incorrect risk estimation (Galán et al., 2019). The constraints are even greater when risk predictions are made for humid tropical regions, where the number of empirical studies is low. Up to now, specific PTE K_d values for soils from the State of São Paulo (southeastern Brazil, humid tropical conditions) have not been completely determined.

The majority of humid tropical soils is highly weathered and are supposed to have a lower PTE sorption capacity compared to temperate soils (Rieuwerts, 2007). Braz et al. (2013a, 2013b) provided a representative database of K_d values for PTE in 21 soils from the eastern Amazon, Brazil's humid equatorial zone. The authors found K_d values lower than those found in major databases, including CETESB (2001), indicating that further K_d data for different tropical soils are required. Another strong argument for defining specific K_d values is given by the Brazilian National Resolution n° 420 (CONAMA, 2009). Prevention values and IV are valid for the whole country. However, the QRV must be determined by each state (CONAMA, 2009) due to the huge diversity of physicochemical and mineralogical composition of the soils, parent materials, climatic conditions, and pedogenetic processes (Nogueira et al., 2018; Fernandes et al., 2018).

Studies on a regional scale are necessary to determine the QRV of PTE in the soils. Since the territory in Brazil is extremely extensive (8,515,767 km²), it makes sense to consider that the PV and IV may also vary according to the huge edaphoclimatic variation. Many authors have commented on the relative lack of data on inorganic contaminants in tropical soils, but the paucity of studies that seek to convert information about PTE sorption into guiding values for use in public policy is even

greater. Recently, a number of research analyses have been developed in Brazil to improve the QRV in various states (Paye et al., 2010; Santos and Alleoni, 2012; Souza et al., 2015; Fernandes et al., 2018; Nogueira et al., 2018), but few studies have been carried out to validate the existing RGV in Brazil, specifically the IV (CETESB, 2016).

An important limitation of the constant K_d model is that it does not address sensitivity to changing conditions and each K_d value is valid for only one set of environmental conditions. Additionally, there is abundant evidence that unique, general or default K_d values can produce significant errors when used to predict the impacts of contaminants. The parametric K_d approach is a robust statistical method that uses a regression equation to define the K_d values as a function of several soil variables or select group of environmental factors (Sheppard, 2011). Many researchers have correlated soil properties [pH, content and type of clay minerals, contents of organic matter and (oxy)hydroxides of Fe, Al, and Mn, and cation exchange capacity (CEC)] with K_d values obtained experimentally for specific soils (Anderson and Christensen, 1988; Bell and Bates, 1988; Buchter et al., 1989; Sheppard and Thibault, 1990; Janssen et al., 1997; Holm et al., 2003; Tipping et al., 2003; Shaheen et al., 2013) or selected from large databases (Sauvé et al., 2000; Carlon et al., 2004).

Our purposes in this study were to determine the solid-liquid partitioning (K_d) of Cd, Co, Cr, Cu, Ni, Pb, and Zn in 30 natural benchmark soils from the State of São Paulo, Brazil's humid tropical zone. Soil samples cover a wide range of chemical, physical, and mineralogical characteristics, enabling regression analysis to identify K_d predictive factors. The hypothesis was that in order to predict K_d relationships must be developed based on data from a broad range of soils and soil properties for them to be sufficiently robust for long-term predictions. Unique K_d values for each PTE were also obtained and critical comparisons to the Environmental Company of the State of São Paulo (CETESB, Brazil) recommendations and to the main international K_d databases were made. Highly significant regression models using simple soil attributes for the refinement of regulatory guiding values, especially intervention values, were obtained.

2. Material and methods

2.1. Soil sampling and characterization

Thirty topsoil samples (A horizon, 0–20 cm) of non-cultivated soils were collected in areas under native vegetation or old reforested vegetation in the State of São Paulo (20–25° S; 44–53° W), southeastern Brazil (Fig. 1). The areas were primarily selected to avoid the collection of soil samples that have undergone recent PTE contamination events. The conduction of the equilibrium partitioning method with soil samples without PTE contamination (at or closely to background levels) is a fundamental premise for the acquisition of K_d values with quality and credibility, since the experimental protocol requires low concentrations of the element of interest.

Due to the extent of anthropogenic disturbances imposed on the environment, there is an evident difficulty in selecting soil sampling areas that really represent PTE background concentrations. Dutch national guidance values were established for soils from various nature reserves throughout the Netherlands (Brus et al., 2009). The State of São Paulo has 4,343,718 ha of native vegetation cover of which 3,810,285 ha belong to the Atlantic Forest biome (dense ombrophylous forest, mixed ombrophylous forest, and seasonal semideciduous forest ecosystems) and 217,513 ha to the Cerrado biome (Brazilian savanna) (SIFESP, 2010). The selected pedotypes have recently been considered adequate benchmarks for PTE natural background values in the State of São Paulo (Nogueira et al., 2018), confirming that they belong to natural areas with low human impact.

Topsoil samples were preferred because they represent the layer of soil that is or will be most subject to PTE contamination events. In addition, topsoil is the most important transfer interface for the

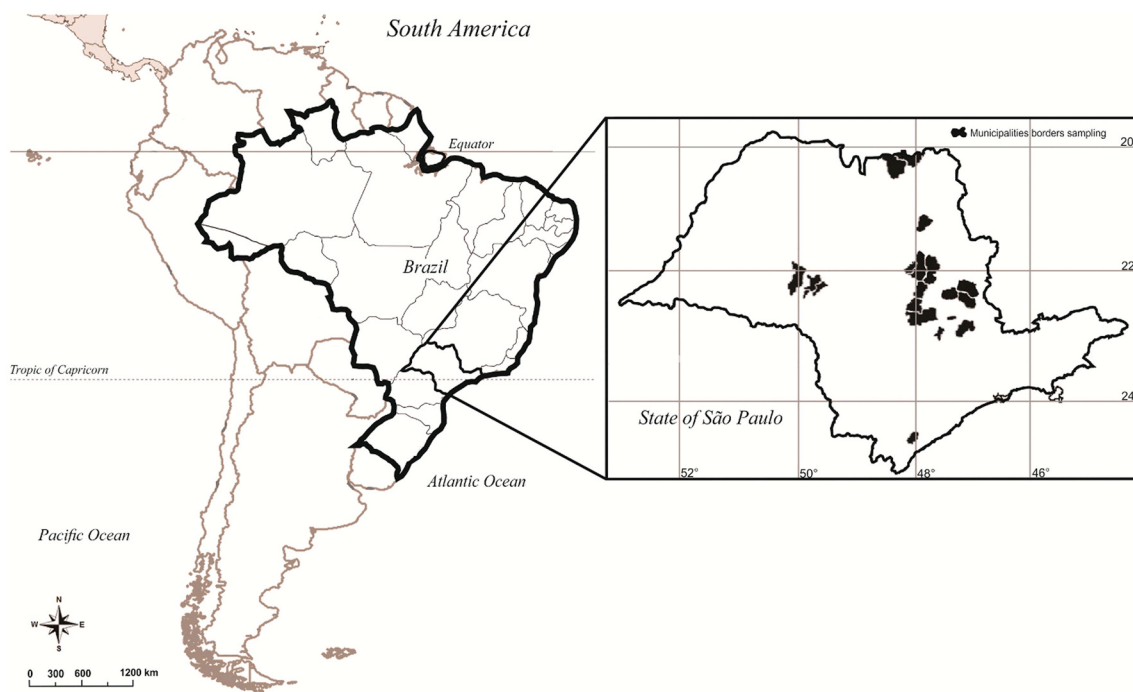


Fig. 1. Location of soil sampling in the State of São Paulo, southeastern Brazil.

accumulation of PTE in the air, plant, and water. For the investigation of PTE surface contamination, the sampling procedures could be limited to the upper layer (0–20 cm) (Sun and Chen, 2016). No specific permission was required for access to the locations or to collect soil samples and the field studies did not involve endangered or protected species. The GPS coordinates of the sampling sites can be found in Table 1.

More serious environmental problems occur in the Metropolitan Region of São Paulo city due to the urban agglomeration [39 municipalities and 21.6 million inhabitants living in about 8000 km² (2700 inhabitants per km⁻²)] and industrial centres with intense goods movement activities. Thus, the State of São Paulo has its own peculiarities as regards the anthropogenic sources and scenarios of PTE point or diffuse contamination, as well as relevant exposure pathways. The safety of State of São Paulo soils is of worldwide strategic importance for agricultural production and food security and for local interest in public health, considering that 52% of the state's municipalities use groundwater exclusively for their public supply and 19% use mixed systems, i.e. part groundwater and part surface water (DAEE, 2013).

According to the Köppen climatological classification, the State of São Paulo has four main kinds of climate, depending on the relief: tropical wet and dry (Aw) along the coastline (20–22 °C; 4154 mm yr⁻¹); humid subtropical (Cwa) on the plateau (20 °C; 1300 mm yr⁻¹); tropical wet and dry (As) in the northwestern region (24 °C; 1000–1250 mm yr⁻¹); and humid subtropical (Cfa) in the southern region (18–20 °C; 1500 mm yr⁻¹).

The natural vegetation is composed of the Atlantic Forest along the shore and surrounding the plateau. The remaining areas present fragments of semideciduous forest and vegetation that include all the formations of the Cerrado biome (Brazilian savanna), such as clean grass fields, grassland with some shrubs, and the cerrado *strictu sensu* (short savanna), which is both arbustive and herbaceous, and the forest formation of "cerradão" (closed savanna approaching a forest) (Soares and Alleoni, 2008).

Many soil orders, such as Oxisols, Ultisols, Alfisols, Entisols, Inceptisols, Histosols, and Mollisols were found in these regions (Rossi, 2017). Thus, the sites were also chosen to ensure the representativeness of the geological, geomorphological, pedological, and typical climatic conditions of the State of São Paulo and to provide a wide range of chemical,

physical, and mineralogical soil properties (Table 1). To avoid contamination with trace elements, soil samples were extracted and prepared using stainless steel instruments (shovel, spatula, sieve), following a standard procedure recommended by CETESB (2001).

A detailed physicochemical and mineralogical characterization was performed on air-dried soil samples passed through a 2 mm mesh sieve, according to official Brazilian procedures (Raij et al., 2001; Camargo et al., 2009; EMBRAPA, 2017) aligned to well known international methods of soil analysis (Sparks et al., 1996; Dane and Topp, 2002; Ulery and Drees, 2008).

Soil pH was determined potentiometrically in both H₂O and 1 mol L⁻¹ KCl solutions (1:2.5 soil:solution ratio) using a combined glasscalomel electrode. The equation $\Delta\text{pH} = \text{pH}_{\text{KCl}} - \text{pH}_{\text{H}_2\text{O}}$ was used to verify the sign of the soil net charge. Effective cation exchange capacity (ECEC = SB + Al) was obtained by the indirect method, as the sum of basic cations (SB = Ca + Mg + K + Na), extracted by ionic exchange resin, and exchangeable aluminium (Al³⁺), extracted by a 1 mol L⁻¹ KCl solution. Calcium and Mg contents were determined by atomic absorption spectroscopy (AAS), Na and K by flame atomic emission spectrometry (FAES), and exchangeable Al by titration with 0.025 mol L⁻¹ NaOH. The content of soil organic carbon (SOC) was quantified by oxidation with potassium dichromate in the presence of sulfuric acid, followed by titration with ammonium Fe²⁺ sulfate (classical Walkley-Black method). Pedogenic iron oxides with high and low crystallinity (Fe_{Na-DCB}) and with low crystallinity (Fe_{Ox}) were extracted, respectively, by sodium dithionite-citrate-bicarbonate (Na-DCB) and by pH 3.0 ammonium acid oxalate (Tam's reagent) in the dark. The Fe contents in the extracts were determined by AAS, and the results were expressed in the form of oxides (Fe₂O₃).

Particle-size distribution analysis of soil samples followed the densimeter method (Bouyoucos modified protocol), after dispersion with 0.015 mol L⁻¹ (NaPO₃)₆.Na₂O + 1 mol L⁻¹ NaOH and treatment with 30% hydrogen peroxide (H₂O₂) for organic matter destruction. Mineralogical examinations of the clay fraction, pre-treated with H₂O₂ and Na-DCB to eliminate organic matter and iron (oxy)hydroxides, respectively, were performed using X-ray diffraction (XRD) analysis of oriented mounts on glass slides. Samples were saturated with either Mg or K. Mg-saturated samples were solvated with glycerol and X-rayed at

Table 1

Taxonomic classification and major chemical, physical, and mineralogical attributes of soils from the State of São Paulo, southeastern Brazil.

Soil Classification		Geographical coordinates		pH	^e ΔpH	^f ECEC	^g Clay	^h OC	ⁱ Fe _{Na-DCB}	^j Fe _{OX}	^k Qualitative mineralogy
^a U.S. Soil Taxonomy	^b Brazilian System (SiBCS)	^c H ₂ O	^d KCl	mmol _c kg ⁻¹	g kg ⁻¹						
Oxisol											
Typic Hapludox-1 (TH-1)	Latossolo Vermelho-Amarelo-1 (LVA-1)	22°19'S 47°10'W	4.5	3.3	-1.2	12.3	181	12.4	19.3	1.7	Kt
Typic Hapludox-2 (TH-2)	Latossolo Vermelho-Amarelo-2 (LVA-2)	22°15'S 47°49'W	4.2	3.2	-1.0	15.5	221	29.9	13.5	0.8	Kt
Typic Hapludox-3 (TH-3)	Latossolo Vermelho-Amarelo-3 (LVA-3)	22°19'S 47°10'W	4.3	3.3	-1.0	11.3	202	16.5	21.3	1.5	Kt
Rhodic Eutrudox-1 (RE-1)	Latossolo Vermelho-1 (LV-1)	22°01'S 47°53'W	6.4	5.1	-1.3	28.4	201	19.4	53.1	3.0	Kt, Gb
Rhodic Eutrudox-2 (RE-2)	Latossolo Vermelho Eutroférico (LVef)	21°05'S 47°08'W	7.3	6.7	-0.6	60.4	684	95.6	185.1	14.8	Kt, Gb
Rhodic Hapludox (RH)	Latossolo Vermelho-2 (LV-2)	22°43'S 47°38'W	4.6	3.4	-1.2	30.6	530	38.1	86.5	6.3	Kt
Rhodic Acrudox (RA)	Latossolo Vermelho Acríferico (LVwf)	21°10'S 47°48'W	4.7	3.7	-1.0	23.7	716	67.4	208.1	19.2	Kt, Gb
Xanthic Hapludox-1 (XH-1)	Latossolo Amarelo-1 (LA-1)	22°15'S 47°49'W	4.8	4.0	-0.8	23.4	222	38.8	19.7	1.3	Kt
Xanthic Hapludox-2 (XH-2)	Latossolo Amarelo-2 (LA-2)	21°57'S 47°59'W	4.4	3.5	-0.9	10.5	342	20.1	42.1	3.4	Kt, Gb
Anionic Acrudox (AA-1)	Latossolo Amarelo Acríferico (LAWf)	20°10'S 48°02'W	4.7	3.7	-1.0	16.9	470	39.9	113.3	7.6	Kt, Gb
Kandiudalfic Eutrudox (KE)	Nitossolo Vermelho Eutroférico (NVef)	21°10'S 47°48'W	5.5	4.7	-0.8	61.1	658	65.6	192.1	15.3	Kt, Gb
Typic Haplaquox (TH-4)	Gleissolo Háplico (GX)	24°43'S 47°52'W	4.7	3.8	-0.9	52.4	532	84.5	27.5	1.7	Kt
Typic Eutraquox (TE)	Gleisolo Melânico (GM)	22°43'S 47°38'W	4.9	3.8	-1.1	50.4	476	213.4	4.9	0.3	Kt
Ultisol											
Arenic Hapludult-1 (AH-1)	Argissolo Vermelho-Amarelo-1 (PVA-1)	22°32'S 47°54'W	5.3	4.3	-1.0	4.9	60	6.7	3.4	0.2	Kt
Arenic Hapludult-2 (AH-2)	Argissolo Vermelho-Amarelo-2 (PVA-2)	22°38'S 47°11'W	5.4	4.7	-0.7	44.6	247	36.8	32.8	3.8	Kt
Arenic Hapludult-3 (AH-3)	Argissolo Vermelho-Amarelo-3 (PVA-3)	22°43'S 47°38'W	6.1	5.5	-0.6	43.5	246	36.6	32.7	2.1	Kt
Arenic Hapludult-4 (AH-4)	Argissolo Vermelho-Amarelo-4 (PVA-4)	22°17'S 49°33'W	5.4	4.3	-1.1	9.4	100	6.8	8.4	0.8	Kt
Typic Hapludult (TH-5)	Nitossolo Háplico (NX)	22°06'S 46°40'W	6.1	5.3	-0.8	66.9	345	54.3	84.5	8.2	Kt, Gb
Arenic Albaquilt (AA-2)	Planoissolo Háplico (SX)	22°43'S 47°38'W	5.6	4.0	-1.6	23.9	204	21.6	18.5	2.2	Kt
Alfisol											
Arenic Hapludalf-1 (AH-5)	Argissolo Vermelho (PV-1)	22°12'S 49°56'W	5.3	4.1	-1.2	8.8	100	7.6	5.3	0.4	Kt, II
Arenic Hapludalf-2 (AH-6)	Argissolo Vermelho-Amarelo-5 (PVA-5)	22°59'S 47°30'W	5.1	4.1	-1.0	21.6	202	17.9	8.7	0.5	Kt, II
Arenic Hapludalf-3 (AH-7)	Luvissolo Crómico (TC)	22°12'S 49°39'W	5.8	3.9	-1.9	7.3	40	9.8	8.2	0.6	Kt, II, HIV
Typic Hapludalf-1 (TH-6)	Argissolo Vermelho-Amarelo-6 (PVA-6)	22°59'S 47°30'W	5.6	5.0	-0.6	68.7	366	41.0	45.7	3.6	Kt, II, HIV
Typic Hapludalf-2 (TH-7)	Argissolo Vermelho (PV-2)	22°06'S 47°07'W	5.7	4.8	-1.1	54.4	427	42.5	51.3	3.9	Kt, II
Entisol											
Typic Quartzipsamment (TQ)	Neossolo Quartzarénico (RQ)	22°32'S 47°54'W	4.4	3.8	-0.6	7.6	80	9.6	2.9	0.3	Kt
Lithic Udortent (LU)	Neossolo Litólico (RL)	22°12'S 49°39'W	5.9	4.8	-1.1	33.0	142	26.2	7.4	0.7	II, HIV
Typic Ustorthent (TU)	Neossolo Regolítico (RR)	22°26'S 49°45'W	6.2	5.1	-1.1	19.2	101	15.5	11.0	0.9	Kt, II
Histosol											
Typic Medifibrist (TM)	Organossolo Háplico (OX)	24°43'S 47°52'W	4.0	3.4	-0.6	57.0	275	197.7	9.2	0.7	Kt
Inceptisol											
Typic Dystrochept (TD)	Cambissolo Háplico (CX)	22°22'S 46°56'W	4.3	3.6	-0.7	22.7	243	29.2	19.2	1.6	Kt
Mollisol											
Typic Argiudoll (TA)	Chernossolo Argilúvico (MT)	22°07'S 47°39'W	5.8	4.1	-1.7	105.5	543	57.8	113.3	7.1	Kt
Range			4.0–7.3	3.2–6.7	-0.6–1.9	4.9–105.5	40–716	6.7–213.4	2.9–208.1	0.2–19.2	
Arithmetic mean		n = 30	5.2	4.2	-1.0	33.2	305	45.3	48.3	3.8	
Median		no outliers	5.2	4.2	-1.0	33.2	305	33.9	28.9	2.4	
Median		n = 30	5.3	4.1	-1.0	23.8	245	33.3	20.5	1.7	
Median		no outliers	5.3	4.0	-0.7	23.8	245	29.6	19.3	1.6	

pH_{H₂O}, ECEC, OC, Fe_{Na-DCB}, and Fe_{OX}: arithmetic mean from three replicates.

Values in bold were considered outliers.

^a United States Keys to Soil Taxonomy (Soil Survey Staff, 2014).^b Brazilian Soil Classification System (SiBCS) (EMBRAPA, 2018).^c pH in H₂O suspension (1:2.5 soil:solution ratio).^d pH in 1 mol L⁻¹ KCl suspension (1:2.5 soil:solution ratio).^e ΔpH = pH_{KCl} - pH_{H₂O}.^f ECEC = effective cation exchange capacity by the summation method (ECEC = Ca + Mg + K + Al, in mmol_c kg⁻¹).^g Particle size analysis by the densimeter method.^h OC = organic carbon content by the Walkley-Black method.ⁱ Fe_{Na-DCB} = pedogenic iron oxides of high and low crystallinity extracted by sodium dithionite-citrate-bicarbonate (Na-DCB).^j Fe_{OX} = pedogenic iron oxides of low crystallinity extracted by pH 3.0 ammonium acid oxalate (Tam's reagent) in the dark.^k Kt = kaolinite; Gb = gibbsite; Il = illite; HIV hydroxy-interlayered vermiculite.

room temperature. K-saturated samples were X-rayed at room temperature and after successive heated to 350 °C and 550 °C. X-ray diffractograms were obtained with a diffractometer (Philips X'pert System) operating at 40 kV and 40 mA using Ni-filtered Cu-K α radiation, at 1.2° 2θ min⁻¹ in the 3–35° 2θ range.

2.2. Laboratory batch sorption experiments

2.2.1. Extract acquisition

Distribution coefficients should be acquired via experiments in which sorption processes control the concentration of a chemical in solution. These conditions are satisfied by batch-type experiments (USEPA, 2008; Soares and Casagrande, 2009), and K_d values from such experiments are considered to be of the highest quality (Bockting et al., 1992; Crommentuijn et al., 1997; USEPA, 1999). This study used the experimental protocol of Harter and Naidu (2001), who proposed a standardization of batch-type experiments to facilitate the comparison of results from different laboratories and/or studies.

Two grams of fine air-dried soil, sieved through 2-mm mesh, was combined with 20 mL of a 10⁻³ mol L⁻¹ NaNO₃ solution (1:10 solid: solution ratio) containing growing initial concentrations of Cd, Co, Cr, Cu, Ni, Pb, and Zn (0.1, 0.5, 1.0, 2.5, and 5.0 mg L⁻¹), in triplicate. The use of high PTE concentrations in sorption tests should be avoided, as this may result in saturation of the binding sites and a decrease in pH (through the displacement of specifically bound protons from surfaces) together with an increase in the ionic strength of the solution (Degryse et al., 2009). Stock solutions of elements were prepared using nitrate salts, Cd(NO₃)₂.4H₂O, Co(NO₃)₂.6H₂O, Cu(NO₃)₂.3H₂O, Ni (NO₃)₂.6H₂O, anhydrous Pb(NO₃)₂, and Zn(NO₃)₂.4H₂O, with the exception of Cr for which sodium dichromate (K₂Cr₂O₇) was used.

The solutions were prepared based on salts certified with high PTE purity, typically exceeding 99.9%. Salts were dissolved in Milli-Q laboratory de-ionized water (electrical conductivity = 0.034 μS cm⁻¹; pH = 6.5; total organic carbon ≤ 5 μg L⁻¹), firstly purified by reverse osmosis and then by application of four ion-exchanger cartridges connected in series. The soil-solution mixture, stored in 50 mL high-density polyethylene Falcon centrifuge tubes, was shaken for 24 h in a horizontal shaker at 120 revolutions min⁻¹. Multiple high-speed centrifuging was used to separate the solid and liquid phases. After shaking, the suspensions were pre-centrifuged at 1875 g for 10 min. A 2 mL aliquot was then placed in Eppendorf tubes and centrifuged at 15,000 g for 30 min. All procedures that posed risks of sample contamination, especially via airborne particles, were carried out in hoods with a horizontal laminar airflow with HEPA filtered incoming air.

2.2.2. Analytical determinations

Analytical determinations were performed in a standard ABNT NBR ISO/IEC 17025 (Brazilian National Standards Organization, 2005) accredited laboratory at the Chemistry and Environment Center (CQMA) of the Nuclear and Energy Research Institute (IPEN). The final PTE concentrations were determined in multi-elemental extracts by high-resolution inductively coupled plasma mass spectrometry (HR-ICPMS - Finnigan MAT Element), interfaced with a low-flow (0.6 mL min⁻¹) concentric nebulizer (Meinhard, Santa Ana, CA, USA) and a Scott-type spray chamber cooled to 6 °C. A typical sensitivity of 1200 MHz/(μg g⁻¹) for ¹¹⁵In was reached.

Solutions of 10 ng g⁻¹ of ¹¹⁵In and ⁷¹Ga were used as internal standards for low and medium resolution, respectively. Samples were subjected to a long rinse of 2 min with 2% (v/v) high purity nitric acid to minimize carry over and clean up the sample introduction system. To avoid adulteration and obtain reliable information (Rodushkin et al., 2010), HR-ICPMS determinations carefully followed all the preparatory steps and instrumental analysis to meet the requirements of multi-elemental analysis at ultra-trace analytical levels.

The RGV should be changed whenever there are new standardizations of the analytical methodology with a lower detection limit

(CETESB, 2001). ICPMS is particularly helpful for measuring trace and ultra-trace concentrations of inorganic elements, such as in the determination of soil background concentrations or of low concentrations applied in the partition method for obtaining K_d from linear isotherms. The HR-ICPMS is an instrumental spectroscopic technique of recognized quality for environmental samples due to its many advantages (multi-element, low detection limits, analytical speed, precision, low matrix and spectral interferences, small volumes, and cost per analysis) (Matusiewicz and Bulska, 2018).

2.2.3. Calculating K_d from sorption isotherms

The PTE concentrations adsorbed by the soil ($[PTE]_{ads}$, mg kg⁻¹) were estimated as the difference between the PTE concentration that was initially added ($[PTE]_0$, mg L⁻¹) and the PTE concentration remaining in the equilibrium solution ($[PTE]_{eq}$, mg L⁻¹), using the expression: $[PTE]_{ads} = [V_{sol} \times ([PTE]_0 - [PTE]_{eq})] / M_{soil}$ in which V_{sol} is the volume of added solution (20 mL = 0.02 L) and M_{soil} = soil mass (2 g = 0.002 kg). This difference (disappearance of the PTE from the solution) may arise through various retention mechanisms (inclusion of the element into crystal structure by co-precipitation or chemical precipitation of a new solid phase at high pH; sorption by inner-sphere surface complex) (Limousin et al., 2007; Sheppard, 2011) which is not an exchange reaction (sorption by outer-sphere surface complex) that is considered a requirement for the theoretically correct use of K_d . In this study, K_d was considered an empirical measure of retention, regardless of mechanism, and then the term "sorption" was used in its broadest sense as proposed by Sposito (1989).

The $[PTE]_{ads}$ was plotted against $[PTE]_{eq}$, to produce the relationship $PTE_{ads} = f(PTE_{eq})$, i.e. the sorption isotherm. The graphs were interpreted using the empirical Freundlich equation, $[PTE]_{ads} = K_f [PTE]_{eq}^n$, in which K_f is the Freundlich coefficient (L kg⁻¹) and n is an empirical, non-dimensional parameter related to the slope of the curve, which expresses the bonding energy. The Freundlich model is that most commonly recommended for experiments with low-solute concentrations, since at the initial portion of the isotherm n is close to unity. When $n = 1$, the Freundlich isotherm is transformed into a C-type linear isotherm and is known as the distribution coefficient model, $K_d = [PTE]_{ads} / [PTE]_{eq}$. Obtaining linear models (without the a intercept) was possible by assuming that the isotherm is a line of zero-origin (Holm et al., 2003; Limousin et al., 2007; Pettenati et al., 2016).

The C-type sorption isotherms were assessed using the statistical significance of the correlation coefficient (r) between $[PTE]_{ads}$ and $[PTE]_{eq}$. Models were considered linear when $r > 0.90$ (significance $p < 0.05$). In those cases, K_d values were extracted directly by the slope coefficients. In extreme cases where isotherms had a non-linear fit (L-type and H-type), which makes the direct derivation of K_d impossible due to the exponential variation in values, K_d was calculated based on the slope of the straight line tangent to the isotherm (Soares, 2004; Braz et al., 2013a).

2.3. Statistical analysis

The raw data of soil attributes and K_d were first subjected to descriptive statistical analysis. The normal distribution of data (Gaussian distribution) was verified by asymmetry and kurtosis coefficients, visual analysis of normal probability histograms, and adherence to the Henry lines, with further confirmation by Shapiro-Wilk (W) and Kolmogorov-Smirnov (KS) tests. Exploratory analysis based on box-and-whisker plots and Cook's distance test was performed on the data set with normal distribution (raw or log-transformed) to detect and exclude potential outliers [data beyond 1.5 times the interquartile ranges (Q3-Q1); Tukey (1977)] to reduce data variability (Brus et al., 2009).

The USEPA (2015b) guidance documents designates outliers defined by tests that assume a normal (Gaussian) distribution, and they should

always be removed from background environmental data (Millard, 2019). An analysis of variance (ANOVA) of the arithmetic mean values of K_d and $\log K_d$, screened for outliers, was performed. When the F-test proved to be significant ($p < 0.05$), data were compared according to Tukey's test ($p < 0.05$). To detect multicollinearity and facilitate its elimination, a correlation matrix was constructed with the values of the physical, chemical, and mineralogical soil attributes. When two independent variables had a correlation coefficient (r) greater than 0.70, it was decided to keep the most easily determined variable in the laboratory for subsequent multiple regression analysis.

Multiple regression analyses were used to identify simple and element-specific mathematical models, with the smallest possible number of independent variables, capable of estimating the parametric values of K_d with variables that were easily determined. Backward stepwise regression was used to reduce the number of explanatory variables in fitting the multiple regression model (Robbins and Daneman, 1999; Sheppard, 2011). Only significance coefficients at $p < 0.10$ were retained in the equations. Multiple regression models were validated only when the variance was homogeneous, distribution was normal, and multicollinearity and outliers were absent (Robbins and Daneman, 1999).

The goodness-of-fit of the mathematical models were assessed by the statistical significance of the coefficients of determination (R^2 and adjusted R^2). The relative importance metric of each predictor variable (partial R^2) as part of the total proportion of variance explained by the model was also provided. In addition, the models were evaluated according to the Akaike Information Criterion (AIC), a method which assumes that the simplest model (lowest AIC value) delivers the best performance for the estimation of new data (Sakamoto et al., 1986). Regression response surface of $\log K_d$ versus soil properties was used to illustrate the extent of the fit. The statistical model for $\log K_d$ was run and the results matched to the $\log K_d$ as determined by batch experiments. The goodness-of-fit of simulated ($Y_{predicted}$) versus measured ($Y_{observed}$) values was tested using the statistical significance of the correlation coefficient (r), at a 95% confidence level. Statistical analyses were carried out with Statistica 10.0 (StatSoft, 2014) and RStudio version 1.2.5001 (R CORE TEAM, 2017) software programs.

3. Results and discussion

3.1. Soil properties

The 30 soils had a broad variation in their chemical, physical, and mineralogical attributes (Table 1). Soil pH varied from extremely acidic (4.0 - TM soil) to slightly basic (7.3 - RE-2 soil) and the arithmetic mean (5.2 ± 0.1) indicated the predominance of acidic soils. All soil samples exhibited negative ΔpH , indicating a negative net charge, and the soils acted predominantly as cation exchangers (Fontes and Alleoni, 2006). The broad variation in soil organic carbon (SOC) [6.7 (AH-1 soil) to 213.4 g kg⁻¹ (TE soil)] reflected the natural vegetation at the sites where the soils were collected and the specific pedogenetic processes of certain soils with high levels of SOC (Typic Eutraquox and Typic Medifibrist soils).

Data on particle size distribution showed a broad variation in clay [40 (AH-3 soil) up to 716 (RA soil) g kg⁻¹], silt [20 (TH-2 soil) up to 448 (AH-6 soil) g kg⁻¹], and sand contents [75 (KE soil) up to 880 (TQ soil) g kg⁻¹], indicating that soil texture varied considerably with a mean prevalence of the loam one. Effective cation exchange capacity (ECEC) varied greatly in value from a very low 4.9 (AH-1 soil) to a high 105.5 (TA soil) mmol_c kg⁻¹. The greatest ECEC values were found in soils with high levels of clay and organic carbon, and in soils with 2:1 phyllosilicates in their mineralogical composition. Contents of pedogenic Fe (oxy) hydroxides with high and low crystallinity (Fe_{Na-DCB}) and of pedogenic Fe poorly crystallized (oxy)hydroxides (Fe_{Ox}) varied from 3.4 (AH-1 soil) to 208.1 (RA soil) g kg⁻¹ and from 0.2 (AH-1 soil) to 19.2 (RA soil) g kg⁻¹, respectively, and were representative of well developed and

weathered soils typical of humid tropical areas (Schaefer et al., 2008).

Kaolinite was the dominant 1:1 layer-type phyllosilicate present in all soil samples except in the Lithic Udortent (LU soil). Diffraction peaks occurred at 0.710 nm and 0.357 nm with subsequent collapse identified in K-saturated samples after thermal treatment at 550 °C. Gibbsite, with typical diffraction peak at 0.458 nm, was detected in most of the Oxisols (RE-1, RE-2, RA, XH-2, AA-1, and KE soils) and in the Typic Hapludult (TH-5 soil). Both minerals are frequent in the clay fraction of highly weathered soils in areas where the annual average rainfall (1500 mm) and the annual average temperature (over 20 °C) caused intensive desilication (Schaefer et al., 2008; Alleoni et al., 2009; Kämpf et al., 2019). Kaolinite can be accompanied by other rare clay minerals, such as hydroxy-interlayered vermiculite (HIV), identified by reflection at 1.43 nm in samples of Typic Hapludalf-1, Arenic Hapludalf-3, and Lithic Udorthent soils. This mineral is not stable under tropical climate conditions and evolves to 1:1 phyllosilicates or to Fe and Al (oxy)hydroxides (Azevedo and Vidal-Torrado, 2019; Kämpf et al., 2019). Although soils from humid tropical regions have undergone an intense weathering process leading to a predominance of kaolinite and Fe and Al (oxy)hydroxides in the clay fraction, significant amounts of 2:1 layer-type minerals, mainly those with Al and Fe interlayer hydroxy polymers, are found in certain situations (Azevedo and Vidal-Torrado, 2019; Kämpf et al., 2019). Entisols, Inceptisols, and Alfisols can contain 2:1 phyllosilicates that are usually found as accessory minerals due to the low amount of mica and vermiculites. The intensity of the XRD reflections evidenced illite, a non-expanding secondary mineral resulting from mica, with diffraction peak at 1.40 nm in K-saturated samples after heating. It was present in the deferrified clay fraction of all the Alfisols (AH-1, AH-6, AH-7, TH-6, and TH-7), but was also observed in Lithic Udorthent and Typic Ustorthent (LU and TU soils) (Table 1). Some representative diffractograms are shown in Fig. 2.

The raw data of the main soil attributes did not show a normal distribution (except pH_{H2O}). Adjusted for the log-normal distribution, soil attributes data did not show outliers. Surprisingly, organic carbon log values of the Typic Eutraquox and Typic Medifibrist (TE and TM soils), considered discrepant and uncommon soils in tropical regions, were not considered outliers (Fig. 3). Empirical relationships derived from multiple regression analysis have provided good descriptions of PTE in typical mineral soils with relatively low levels of organic matter (i.e. with loss-on-ignition values of 10% or less), but there do not appear to have been applications to more organic-rich soils (Tipping et al., 2003).

For practical proposals of soil and groundwater quality evaluation, the risk assessment models have used a standard and hypothetical soil type to extrapolate toxicity and exposure data. Among the soil characteristics, contents of organic matter and clay are directly applied to the generation of IV, while the use of soil pH for site-specific assessment has been considered (Otte et al., 2001). For soils frequently found in the Netherlands, the ranges of pH, and contents of clay and organic matter have been, respectively, 3.2–7.4, 20–500 g kg⁻¹, and 0–900 g kg⁻¹. The CSoIL model adopts a default soil with the following characteristics: pH_{KCl} 6.0, clay content of 250 g kg⁻¹, and organic matter content of 100 g kg⁻¹ (Brand et al., 2007).

The intervals of pH from 4.6 to 5.8, organic matter content (organic carbon $\times 1.724$) between 28.4 and 93.6 g kg⁻¹, and clay content between 181 and 470 g kg⁻¹ better represented our soil group (Fig. 3). Then, according to the median values (Table 1) and disregarding outliers, a standard soil for humid tropical edaphoclimatic conditions could have pH_{H2O} 5.3, clay content of 245 g kg⁻¹, and organic matter content of 51 g kg⁻¹ and should be considered for inclusion in CETESB's current spreadsheet model database for use under the São Paulo State conditions. The organic matter content typical of natural soils should be used with caution, as it may not completely reflect the organic matter content observed in Brazilian agricultural soils.

Soil organic matter (SOM) stocks to a depth of 30 cm on Brazilian sites with native vegetation in the absence of significant disturbances (considered a valuable baseline for evaluating the effect of land-use

change in soil C stocks for Brazil) ranged from 8.62 g kg^{-1} to 239.6 g kg^{-1} . More than 75% of the areas exhibited $17.2\text{--}34.4 \text{ g kg}^{-1}$ of soil organic matter (Bernoux et al., 2002). In another study, Assad et al. (2013) showed that areas with native vegetation (Cerrado, Atlantic Forest, and Pampa) had SOM stocks at a soil depth of 30 cm equal to 36.7 g kg^{-1} , with SOM losses of 6.65 g kg^{-1} in crop-livestock systems and 6.33 g kg^{-1} in pasture soils.

3.2. Modeling of PTE sorption isotherms

Three types of isotherms (L, H, and C) (Hinz, 2001; Limousin et al., 2007) were used to fit the experimental sorption results depending on the soils and PTE (Fig. 4). While the isotherms do not indicate the primary sorption mechanism, the shape of the curves, and especially their initial slope, provide hints about the reaction (Hinz, 2001; Soares and Casagrande, 2009).

Approximately 24% of the experimental isotherms were L-type. When the sorption of PTE to a surface begins to decrease as sites become occupied, the pattern is described as asymptotic type-L isotherm. Its initial slope does not increase with the concentration of PTE in soil solution. Isotherms of this kind adequately described the sorption of Cr for 26 soils (Table 2). In approximately 30% of cases, L-type isotherms described the sorption of Cd and Zn. Specifically in these cases, the K_d values were obtained as the slopes of the tangent lines to the isotherms (Soares, 2004; Braz et al., 2013b). The K_d values for AH-1, TQ, and TC soils, regardless of PTE, were also obtained by this method. The low K_d values obtained for these soils were attributed to its low ECEC and low clay and OC contents (Table 1), and not to the adjustment to the L-type isotherm. Sorption of Co, Cu, Ni, and Pb were poorly described by L-type isotherms. Adjustments to L-type isotherms resulted in intervals with low K_d values for Cd ($7\text{--}221 \text{ L kg}^{-1}$), Co ($19\text{--}64 \text{ L kg}^{-1}$), Cu ($105\text{--}220 \text{ L kg}^{-1}$), Ni (47 L kg^{-1}), and Zn ($8\text{--}227 \text{ L kg}^{-1}$).

The H-type curves are extreme versions of the L-curve isotherms caused by specific sorption. Its characteristically large initial slope is associated with the high affinity of the soil to the element by inner-sphere surface complexation. H-type curves were clearly identified in 28% of the sorption isotherms, particularly in describing the retention of Cu and Pb (Table 2). The sorption of cations more strongly retained by the soil, such as Cu and Pb, tend to be represented by H-type isotherms (Harter, 1983).

Copper has a greater capacity for sharing electrons with functional groups with electron deficiency, primarily the carboxyl and OH phenolic functional groups of humic substances and the hydroxylated groups of the broken edges of kaolinite and surface of Fe and Al oxy(hydroxy)oxides

(Silveira et al., 2002; Silveira and Alleoni, 2003; Mouta et al., 2008). This probably explains the fact that the Cu sorption had been adjusted for type-C or type-H isotherms (Table 2). The sharp initial inclination of the H-type isotherm shown by AA-1, TH-5, TH-6, LU, TU, and TE soils suggested a high level of affinity also with Cd and Co, as a result either of surface complexation mechanisms of the inner-sphere type or significant sorption processes mediated by van der Waals interactions (Sposito, 1989; Bradl, 2004). The H-type isotherms have resulted in intervals with a wide range of K_d values for Co ($125\text{--}2085 \text{ L kg}^{-1}$), Cu ($416\text{--}3044 \text{ L kg}^{-1}$), and Pb ($379\text{--}6368 \text{ L kg}^{-1}$).

Approximately 47% of the isotherms were C-type (Table 2). The C-type isotherm is characterized by an initial slope that remains independent of PTE concentration until the maximum possible sorption is achieved. This isotherm is a curve with a constant slope that directly fits the distribution coefficient model. It is produced either by a constant partitioning of an element between the interfacial region and soil solution, or by a proportional increase in the amount of adsorbing surface as the concentration of element increases. These isotherms describe the sorption in experimental conditions at low solute concentration. If higher concentrations had been added, certainly the isotherm would reach its point of curvature, tending to the asymptotic performance of the L-type isotherm (Hinz, 2001; Limousin et al., 2007).

The C-type isotherms were predominant in describing the sorption of PTE by Ultisols, Alfisols, and, especially, Oxisols. However, sorption of PTE by Entisols and the Cr sorption were not fitted by C-type isotherms. About 87% of Ni sorption isotherms, 70% of Co, 53% of Pb, and 50% of Cu were C-type. The highest range of K_d (L kg^{-1}) for Cd (100–2850), Cu (280–3442), Ni (7–998), Pb (121–7020), and Zn (5–1037) were observed from adjustments to C-type isotherms.

Because K_d is theoretically derived from a linear model, the calculation was based on the equation of the tangent line to the curve (L-type isotherms) when the correlation coefficient (r) was less than 0.9. Apparently adjustments to L-type isotherms can result in underestimated values for K_d , although the calculation by the tangent line inclination to isotherm has been considered an artifice to obtain K_d values under similar conditions to those with C-type and H-type isotherms (i.e., with the n exponent as close as possible to unity). Thus, it was assumed that the type of sorption isotherm did not affect the K_d values. Models with correlation coefficients (r) greater than or equal to 0.9 were considered linear and suitable to directly provide the K_d value. This pattern was typical for C- and H-type isotherms to fit Cu and Pb sorption. Outliers were also predominantly observed from adjustments to C- and H-type isotherms (Table 2).

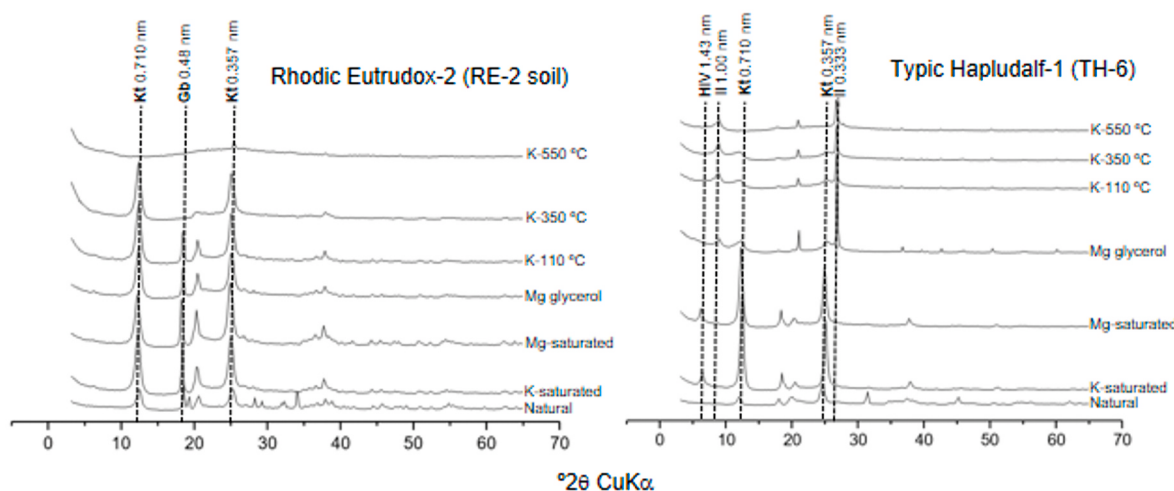


Fig. 2. X-ray diffractograms of oriented clay fraction of some soils from State of São Paulo, southeastern Brazil. Kt - kaolinite; Gb - gibbsite; HIV - hydroxy-interlayered vermiculite; Il - illite.

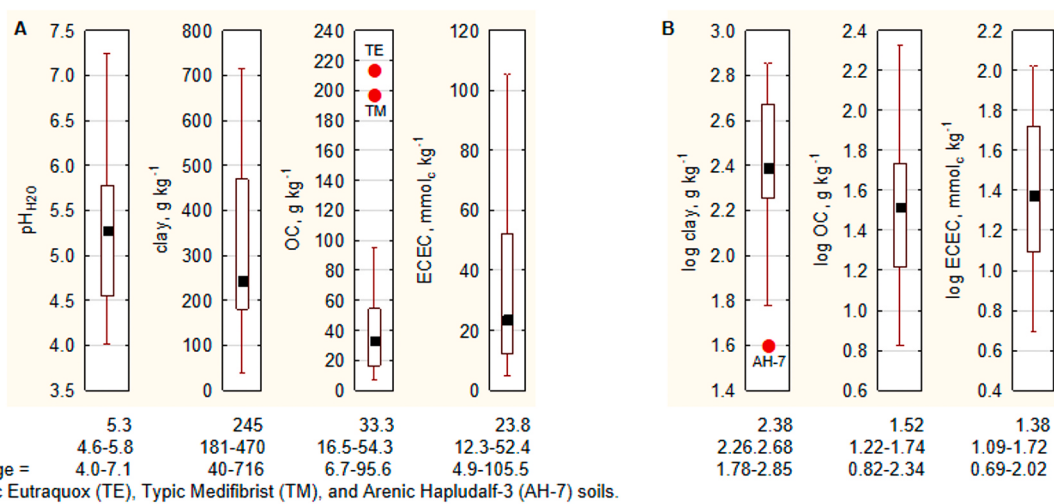


Fig. 3. Range and distribution of the main soil attributes used to estimate K_d of PTE for the edaphoclimatic conditions of the State of São Paulo, southeastern Brazil. ECEC = effective cation exchange capacity by the summation method (ECEC = Ca + Mg + K + Al, in mmol_c kg⁻¹); clay content by the hydrometer method (g kg⁻¹); OC = organic matter content by the Walkley-Black method (g kg⁻¹); pH_{H₂O} = in H₂O suspensions (1:2.5 soil:solution ratio); A = raw data; B = log-transformed data.

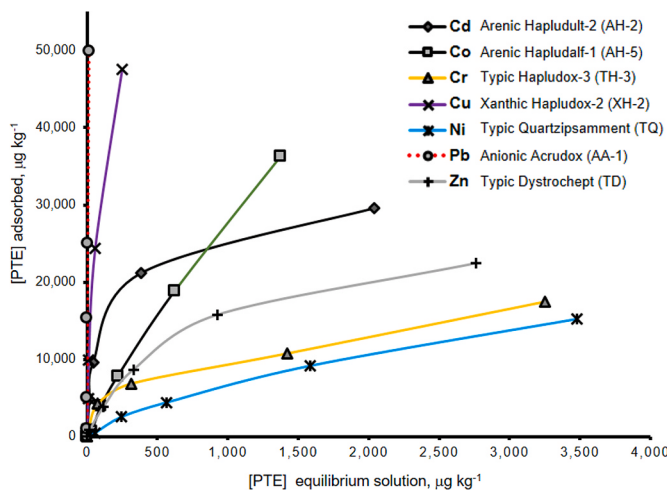


Fig. 4. Three main types of isotherms adjusted to the sorption of PTE by some soils from State of São Paulo, southeastern Brazil. Sorption isotherms were used to calculate K_d of PTE and were obtained from batch-type experiments (1:10 soil:solution ratio, 10⁻³ mol L⁻¹ NaNO₃ solution as supporting electrolyte and 24 h stirring at 24 °C) with different soils. Type-C isotherms: Ni and Co; Type-H isotherms: Cu and Pb; Type-L isotherms: Cd, Cr, and Zn.

3.3. Distribution coefficients (K_d) values

3.3.1. Range of variation and outliers

The raw data for the K_d values did not match the standard Gaussian normal distribution. K_d values exhibited a log-normal distribution pattern, with or without the elimination of outliers. The observation of absolute values allowed for a better perception of the wide ranges in K_d variation. The smallest variations in K_d values were recorded for Pb (one order of magnitude – 121 to 7020 L kg⁻¹), Cu (one order of magnitude – 105 to 4598 L kg⁻¹), and Ni (two orders of magnitude - 6 to 998 L kg⁻¹), while variations indicating four orders of magnitude were observed for Cd (7–14,339 L kg⁻¹), Co (2–34,473 L kg⁻¹), and Cr (1–21,267 L kg⁻¹). The K_d values for Zn were between 5 and 123,849 L kg⁻¹, with a variation of five orders of magnitude (Table 2).

Several researchers (Bucher et al., 1989; Sheppard and Thibault, 1990; Janssen et al., 1997; Sauvé et al., 2000; Gil-García et al., 2009; Braz et al., 2013a, 2013b) have reported an even wider range of variation in K_d values for several elements (Table 3). The cases with the

greatest variation resulted from some outliers (Fig. 5). Rhodic Eutrudox-2 (RE-2 soil) presented high K_d values that were outliers for Cd (14,339 mg kg⁻¹), Co (5647 mg kg⁻¹), Ni (998 mg kg⁻¹), and Zn (123,849 mg kg⁻¹). Outliers of K_d values for Co (2085 mg kg⁻¹), Cr (21,267 mg kg⁻¹) and Cu (4598 mg kg⁻¹) were also observed in Typic Argiudoll (TA soil). Both RE-2 and TA soils present outliers for contents of crystalline and poorly crystallized Fe (oxy)hydroxides (Table 1). Even with outliers for contents of Fe_{Na}-DCB and Fe_{ox}, the RA soil resulted in anomalous K_d for Cr only (4178 mg kg⁻¹). Outliers for organic carbon (TE and TM soils, Table 1) did not result in anomalous K_d values, except for Cr (19,988 mg kg⁻¹) in TE soil. The lowest K_d values were recorded in soils with low contents of clay and organic carbon (TH-1, AH-1, and TQ soils) (Tables 1 and 2). The majority of the highest values were considered outliers, and were mostly associated with the Rhodic Acruodox (Cd, Ni, Pb, and Zn) and with the Typic Argiudoll (Cr and Cu) soils, probably due to their high pH and high ECEC, respectively (Table 1). The logarithmic conversion of the data reduced the number of outliers (Fig. 5). Outliers of log K_d were identified for the following PTE and soils (Fig. 5): Co – Arenic Hapludalf-2 (AH-6) and Arenic Hapludalf-3 (AH-3); Cr - Arenic Hapludalf-1 (AH-1), Kandiudalfic Eutrudox (KE), Typic Eutraquox (TE), and Typic Argiudoll (TA); Zn - Rhodic Eutrudox-2 (RE-2).

The ANOVA tests demonstrate that the effect of the nature of PTE on their chemical partition in soils was highly significant ($p < 0.01$). According to Tukey's test ($p < 0.05$) from amongst the absolute arithmetic means (after excluding the outliers), the K_d of Pb was the highest, followed by those of Cu, and Cd (Table 2 and Fig. 5). Mean K_d values of Co, Cr, Ni, and Zn were not statistically different. According to the mean K_d values, the follow order of affinity was observed: Pb (2645 L kg⁻¹) > Cu (1142 L kg⁻¹) > Cd (684 L kg⁻¹) > Ni (186 L kg⁻¹) = Zn (185 L kg⁻¹) = Co (143 L kg⁻¹) = Cr (108 L kg⁻¹). As in other studies (Allison and Allison, 2005; Braz et al., 2013a, 2013b), the median values of K_d were considered the best central tendency measure, and were used to establish the following order of affinity: Pb (2132 L kg⁻¹) > Cu (772 L kg⁻¹) > Cd (221 L kg⁻¹) > Ni (112 L kg⁻¹) > Zn (90 L kg⁻¹) > Cr (85 L kg⁻¹) > Co (63 L kg⁻¹) (Table 4).

The sorption selectivity sequence of PTE by soils could be determined at selected values of K_d to obtain one comparable value for each element and each soil. A high K_d value indicates high element retention by the solid phase through chemical reactions, leading to low element bioavailability (Anderson and Christensen, 1988; Shaheen et al., 2013). Conversely, a low K_d value indicates that a high amount of the element remains in the solution. The selectivity sequence

Table 2Raw and log-transformed K_d values of PTE in representative soils from the State of São Paulo, southeastern Brazil.

Soil	Cd	Co	Cr	Cu	Ni	Pb	Zn	Cd	Co	Cr	Cu	Ni	Pb	Zn
	K_d (L kg^{-1})	$\log_{10}K_d$ (L kg^{-1})												
Oxisol														
Typic Hapludox-1 (TH-1)	28 (L)	3 (C)	99 (L)	220 (L)	6 (C)	130 (C)	5 (C)	1.45	0.48	2.00	2.34	0.78	2.11	0.70
Typic Hapludox-2 (TH-2)	31 (L)	6 (C)	85 (L)	480 (H)	21 (C)	364 (C)	7 (C)	1.49	0.78	1.93	2.68	1.32	2.56	0.85
Typic Hapludox-3 (TH-3)	203 (C)	81 (C)	55 (L)	496 (C)	7 (C)	1715 (C)	423 (H)	2.31	1.91	1.74	2.70	0.85	3.23	2.63
Rhodic Eutrudox-1 (RE-1)	1421 (C)	304 (H)	43 (L)	1363 (H)	265 (C)	3506 (H)	1947 (C)	3.15	2.48	1.63	3.13	2.42	3.54	3.29
Rhodic Eutrudox-2 (RE-2)	14,339 (H)	5647 (C)	257 (L)	1097 (H)	998 (C)	7020 (C)	123,849 (H)	4.16	3.75	2.41	3.04	3.00	3.85	5.09
Rhodic Haplodox (RH)	140 (C)	39 (C)	930 (L)	1751 (C)	101 (C)	1495 (C)	66 (H)	2.15	1.59	2.97	3.24	2.00	3.17	1.82
Rhodic Acrudox (RA)	177 (H)	62 (C)	4178 (H)	1749 (H)	111 (C)	5234 (C)	144 (C)	2.25	1.79	3.62	3.24	2.05	3.72	2.16
Xanthic Hapludox-1 (XH-1)	449 (H)	101 (C)	1000 (L)	453 (C)	134 (C)	1238 (C)	97 (C)	2.65	2.00	3.00	2.66	2.13	3.09	1.99
Xanthic Hapludox-2 (XH-2)	23 (L)	9 (C)	304 (L)	772 (C)	13 (C)	407 (C)	13 (L)	1.36	0.95	2.48	2.89	1.11	2.61	1.11
Anionic Acrudox (AA-1)	179 (H)	57 (C)	7566 (H)	2222 (H)	58 (C)	3703 (H)	107 (H)	2.25	1.76	3.88	3.35	1.76	3.57	2.03
Kandiudalfic Eutrudox (KE)	1641 (C)	656 (C)	9990 (L)	3371 (C)	957 (C)	6514 (C)	7349 (H)	3.22	2.82	4.00	3.53	2.98	3.81	3.87
Typic Haplaquox (TH-4)	145 (C)	64 (L)	354 (H)	529 (C)	123 (C)	2709 (H)	82 (L)	2.16	1.81	2.55	2.72	2.09	3.43	1.91
Typic Eutraquox (TE)	226 (H)	62 (C)	19,988 (L)	3044 (H)	113 (C)	2356 (H)	81 (L)	2.35	1.79	4.30	3.48	2.05	3.37	1.91
Ultisol														
Arenic Hapludult-1 (AH-1)	118 (L)	19 (L)	1 (L)	469 (C)	61 (C)	1185 (H)	42 (L)	2.07	1.28	0.06	2.67	1.79	3.07	1.62
Arenic Hapludult-2 (AH-2)	221 (L)	108 (C)	4 (L)	280 (C)	109 (C)	859 (C)	144 (C)	2.34	2.03	0.60	2.45	2.04	2.93	2.16
Arenic Hapludult-3 (AH-3)	2217 (C)	11,755 (C)	6 (L)	1114 (H)	458 (H)	3895 (C)	675 (H)	3.35	4.07	0.78	3.05	2.66	3.59	2.83
Arenic Hapludult-4 (AH-4)	774 (H)	268 (C)	100 (L)	1293 (C)	196 (C)	3488 (C)	129 (H)	2.89	2.43	2.00	3.11	2.29	3.54	2.11
Typic Hapludult (TH-5)	1207 (C)	570 (H)	377 (L)	715 (H)	558 (C)	2683 (H)	8037 (H)	3.08	2.76	2.58	2.85	2.75	3.43	3.91
Arenic Albaquult (AA-2)	302 (H)	90 (C)	106 (L)	1605 (C)	174 (C)	4304 (H)	204 (L)	2.48	1.95	2.03	3.21	2.24	3.63	2.31
Alfisol														
Arenic Hapludalf-1 (AH-5)	39 (L)	27 (C)	87 (L)	317 (C)	35 (C)	733 (C)	35 (C)	1.59	1.43	1.94	2.50	1.54	2.87	1.54
Arenic Hapludalf-2 (AH-6)	2850 (C)	34,473 (H)	8 (L)	1628 (C)	482 (C)	4542 (C)	2221 (H)	3.45	4.54	0.90	3.21	2.68	3.66	3.35
Arenic Hapludalf-3 (AH-7)	176 (L)	31 (C)	34 (L)	519 (C)	47 (L)	965 (H)	52 (L)	2.25	1.49	1.53	2.72	1.67	2.98	1.72
Typic Hapludalf-1 (TH-6)	1500 (C)	572 (H)	8 (L)	1922 (H)	444 (H)	3222 (H)	2974 (H)	3.18	2.76	0.90	3.28	2.65	3.51	3.47
Typic Hapludalf-2 (TH-7)	1309 (C)	289 (C)	202 (L)	3442 (C)	402 (C)	5687 (H)	1037 (C)	3.12	2.46	2.31	3.54	2.60	3.75	3.02
Entisol														
Typic Quartzipsament (TQ)	7 (L)	2 (C)	54 (L)	105 (L)	8 (C)	121 (C)	8 (L)	0.85	0.30	1.73	2.02	0.90	2.08	0.90
Lithic Udortent (LU)	655 (H)	125 (H)	50 (L)	331 (C)	212 (C)	1907 (H)	187 (L)	2.82	2.10	1.70	2.52	2.33	3.28	2.27
Typic Usthorment (TU)	654 (H)	132 (H)	2 (L)	841 (H)	183 (H)	1574 (H)	277 (L)	2.82	2.12	0.30	2.92	2.26	3.20	2.44
Histosol														
Typic Medifibrust (TM)	100 (C)	27 (C)	115 (H)	416 (H)	58 (C)	1049 (C)	32 (L)	2.00	1.43	2.06	2.62	1.76	3.02	1.51
Inceptisol														
Typic Dystrochept (TD)	19 (L)	16 (C)	139 (L)	574 (H)	32 (C)	379 (H)	32 (L)	1.28	1.20	2.14	2.76	1.51	2.58	1.51
Mollisol														
Typic Argiudoll (TA)	3019 (C)	2085 (H)	21,267 (L)	4598 (H)	786 (C)	6368 (H)	569 (C)	3.48	3.32	4.33	3.66	2.90	3.80	2.76
Arithmetic mean		n = 30	1139	1923	2247	1257	238	2645	5028	2.47	2.06	2.15	2.94	2.04
		no outliers	684bc	143c	108c	1142b	185c	2645a	185c	2.47	1.90	1.99	2.94	2.04
Median		n = 30	223	85	103	807	118	2131	137	2.35	1.93	2.01	2.91	2.07
		no outliers	221	63	85	772	112	2131	90	2.35	1.86	2.00	2.91	2.07

Letters in parentheses indicate the type of sorption isotherm (L, H, or C).

Arithmetic means followed by the same letter did not differ according to Tukey's test ($p < 0.05$).

Values in bold were considered outliers.

$\text{Pb} > \text{Cu} > \text{Hg} > \text{Cr} > \text{Cd} \cong \text{Co} > \text{Ni} > \text{Zn}$ was obtained by [Braz et al. \(2013a, 2013b\)](#), based on K_d values of soils from the Brazilian Amazon. Other studies on Brazilian soils ([Gomes et al., 2001](#); [Matos et al., 2001](#)) showed high variation in the affinity sequence. The sorption selective sequence is an important measure of retention energy and usually reflects the facility with which elements form high-energy inner-sphere complexes. Normally, the sequence depends on the intrinsic chemical properties of each element, such as the electronic configuration, the number of unpaired electrons of the outermost electron shell, valence, ionic radius, electronegativity, and first hydrolysis constant (pK) ([McBride, 1989](#); [Covelo et al., 2007](#)). For example, based on the first hydrolysis constant (pK), [Sposito \(1989\)](#) suggested the sequence $\text{Pb} (7.7) > \text{Cu} (7.7) \gg \text{Zn} (9.0) > \text{Co} (9.0) > \text{Ni} (9.9) > \text{Cd} (10.1)$. According to electronegativity, the most likely sequence is $\text{Cu} (1.9) > \text{Pb} (1.8) = \text{Ni} (1.8) > \text{Cd} (1.7) > \text{Cr} (1.6) = \text{Zn} (1.6)$ ([Covelo et al., 2007](#)). Relative PTE mobility identified by [Kim et al. \(2015\)](#) [$\text{Cr(VI)} > \text{Cd} > \text{Ni} > \text{Zn} > \text{Cu} > \text{Pb} = \text{Cr(III)}$] corresponds to both the sequences of pK values of ion hydroxides and those of the stability constant of metal-organic complexes, by which PTE could be grouped as follows: high mobility - Cd, Ni, and Zn; low mobility - Cu, Cr (III), and Pb. Due to the chemical characteristics of Pb and Cu (relatively high electronegativity, lower pK, small hydrated radius, and electronic structure), these metals are sorbed more strongly than other elements, i.e. Cd, Ni, and Zn, thus showing lower lability in the soils and posing less of a threat to groundwater systems and growing plants. The differences in affinity sequences observed in different studies ([Table 4](#)) are indeed caused by the effect of element interaction with different soils, which in turn exhibit chemical, physical, and mineralogical differences that are distinguished further by the effect of climatic region.

3.3.2. Comparison with other K_d databases

Comparing results of K_d with other studies allows variations among soils, elements, and regions ([Tables 3 and 4](#)) to be recorded. However, the comparison can be problematic and should be cautious, primarily due to the different experimental protocols ([Koning et al., 2000](#)). Field-based K_d of metals (Cd, Cr, Cu, Ni, Pb, and Zn) for 20 Dutch soils were between 6 (Zn) and 67,856 (Pb) L kg^{-1} ([Janssen et al., 1997](#)). Wider ranges of K_d values (L kg^{-1}) for the same elements were observed by [Sauvé et al. \(2000\)](#) in the data of a literary compilation of studies on temperate soils: Cd, 0.44–192,000 L kg^{-1} ; Cr, 125–65,609 L kg^{-1} ; Cu, 6.8–82,850 L kg^{-1} ; Ni, 8.9–256,842 L kg^{-1} ; Pb, 60.5–2,304,762 L kg^{-1} ; and Zn, 1.4–320,000 L kg^{-1} . In this case, K_d values were derived from experiments in which total metal contents and the corresponding soluble proportions were obtained via acid digestion. Thus, these K_d values

could have been higher because they also include the part of the PTE fraction that belongs to the crystalline structure of the mineral and that (in theory) is not in equilibrium with the PTE fraction in solution.

Distribution coefficients from batch type experiments and from sorption isotherms consider only the portion of PTE that is in equilibrium with the solution phase. Nevertheless, researchers who used batch sorption experiments to obtain K_d values of Cd, Co, Cr, Cu, Ni, Pb, and Zn of soils from the United States ([Buchter et al., 1989](#)) also observed a wide range of variation, such as from 2.1 (Zn) to 43,151,907 (Pb) L kg^{-1} . For Brazilian soils from the eastern Amazon, a narrow range of K_d values was found for Pb (196–5572 kg L^{-1}), Cu (51–7368 kg L^{-1}), and Ni (5–524 kg L^{-1}). The wider ranges were obtained for Cd (6–2471 kg L^{-1}), Co (3–4604 kg L^{-1}), Cr (3–1811 kg L^{-1}), and Zn (1.4–7933 kg L^{-1}) ([Braz et al., 2013a; 2013b](#)). Disregarding the outliers ([Table 2](#)), the ranges of K_d values for Cd, Ni, Pb, and Zn were very similar to those found by [Braz et al. \(2013a, 2013b\)](#), which in turn had higher K_d values for Co, Cr and Cu, under identical experimental conditions for this study.

According to the median K_d results (Cd – 221 kg L^{-1} , Co – 81 kg L^{-1} , Cr – 85 kg L^{-1} , Cu – 574 kg L^{-1} , Ni – 123 kg L^{-1} , Pb – 1715 kg L^{-1} , Zn – 102 kg L^{-1}), and the range of variation in K_d values found in this study (Cd 7–2217 kg L^{-1} , Co 2–2085 kg L^{-1} , Cr 1–377 kg L^{-1} , Cu 105–3442 kg L^{-1} , Ni 6–558 kg L^{-1} , Pb 121–7020 kg L^{-1} , Zn 5–1037 kg L^{-1}) ([Table 2](#)), disregarding the outliers, K_d values of [CETESB \(2001\)](#) (Cd – 190 kg L^{-1} , Co – 120 kg L^{-1} , Cr – 4400 kg L^{-1} , Cu – 540 kg L^{-1} , Ni – 560 kg L^{-1} , Pb – 2400 kg L^{-1} , Zn – 250 L kg^{-1}) result in correct estimates of the risk associated with the retention of Cd, Co, Cu, Pb, and Zn. The K_d values for Cd, Cu, and Ni ([CETESB, 2001](#)) were, respectively, 3.2-fold smaller, 1.7-fold larger, and 3.3-fold smaller than those obtained in our study. The major discrepancy was observed between the K_d values of Cr. The value obtained in this study (109 L kg^{-1}) was 40-fold lower than [CETESB \(2001\)](#) (4400 L kg^{-1}). The K_d values that appears in the recent USEPA's generic tables for regional screening levels ([USEPA, 2019](#)) (Cd – 75 L kg^{-1} , Co – 45 L kg^{-1} , Cr(III) – 19 L kg^{-1} , Cu – 35 L kg^{-1} , Ni – 65 L kg^{-1} , and Zn – 62 L kg^{-1}) are lower than our mean or median values, with the exception of K_d for Pb (8100 L kg^{-1}).

Our median results for K_d of Cr (85 L kg^{-1}) showed that the value of [CETESB \(2001\)](#) (4400 L kg^{-1}) could be high, and inappropriate for humid tropical soils. High K_d values for Cr ranging from 4786 to 14,454 L kg^{-1} have been presented in several studies ([Sauvé et al., 2000](#); [Otte et al., 2001](#); [Allison and Allison, 2005](#)), including 1,800,000 L kg^{-1} for K_d of total Cr published by [USEPA \(2019\)](#) ([Table 4](#)); however, in our study, K_d values for Cr above 930 L kg^{-1} were considered outliers ([Table 2](#)). The K_d of [CETESB \(2001\)](#) for Cr is similar to those found in [Sauvé et al. \(2000\)](#) and [Otte et al. \(2001\)](#) ([Table 4](#)).

Table 3

Range of variation for K_d of PTE in this study and as reported in the scientific literature.

Reference	Cd	Co	Cr	Cu	Ni	Pb	Zn
L kg^{-1}							
^a This study	7–14,339	2–34,473	1–21,267	105–4598	6–998	121–7020	5–123,849
^b Buchter et al. (1989)	5.4–755	2.5–363	3.6–63	53–6353	3.4–336	136–43,151,907	2.1–774
^c Sheppard and Thibault (1990)	7–962	100–9700	2.2–1000	–	–	3500–59,000	3.6–11,000
^d Janssen et al. (1997)	21–18,263	–	524–24,217	25–4318	115–5749	916–67,856	6–6762
^e Sauvé et al. (2000)	0.44–192,000	–	125–65,609	6.8–82,850	8.9–256,842	60.5–2,304,762	1.4–320,000
^f Gil-Garcia et al. (2009)	2–7000	2–103,595	1–7943	76–2733	3–7250	–	0.9–153,070
^g Braz et al. (2013a, 2013b)	6–2471	2.7–4604	2.5–1811	50.5–7368	4.7–524	196.4–5572	1.4–7933

^a Experimental data for 30 soils from southeastern Brazil, using batch adsorption experiments.

^b Experimental data for 11 American soils, using batch adsorption experiments.

^c Literature data compendium for Canadian loam soils (number of soils and methods of obtaining K_d were not reported).

^d Field-based K_d for 20 Dutch soils, determined by calculating the ratio of the amount of metal extracted by concentrated HNO_3 to the metal concentration in the pore water ([M]solid phase/[M]pore water).

^e Literature data compilation of 70 studies (number of soils was not reported; compiled data from experimental results of K_d obtained from the relation between soil total metal content (using some sort of acid digestion) and concentration of dissolved metal in solution (using the ratio [M]total/[M]dissolved)).

^f Literature data compilation come from field and laboratory experiments considering the scenario of soils contaminated by radioisotopes, and from references mostly from 1990 onwards.

^g Experimental data for 21 soils from eastern Amazon, Brazil, using experimental procedures identical to those of this study.

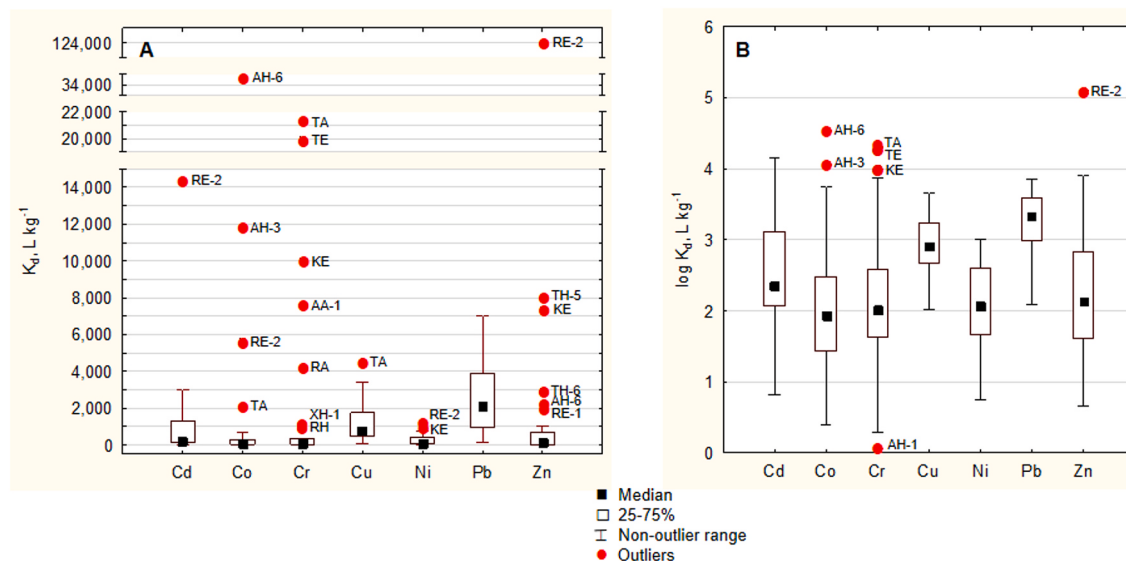


Fig. 5. Range and distribution of K_d of Cd, Co, Cu, Cr, Ni, Pb, and Zn in soils from State of São Paulo, southeastern Brazil. A = raw data; B = log-transformed data.

Table 4

Distribution coefficients (K_d) of PTE and adsorption selectivity sequence based on K_d obtained in this study and in other datasets.

Reference	Measure of central tendency	Cd	Co	Cr	Cu	Ni	Pb	Zn	Adsorption selectivity sequence
		$L \text{ kg}^{-1}$							
This study	mean	612	120	109	917	168	2149	195	Pb > Cu > Cd > Ni > Zn > Cr > Co
	median	221	81	85	574	123	1715	102	Pb > Cu > Cd > Zn > Ni > Co > Cr
Buchter et al. (1989)	mean	59	37	*11	316	36	3388	48	Pb > Cu > Cd > Zn > Co > Ni > Cr
^a Van den Berg and Roels [cited by Otte et al. (2001)]	mean	191	120	**14,454	537	562	2399	251	Cr > Pb > Ni > Cu > Zn > Cd > Co
^b Otte et al. (2001)	mean	2570	120	***4786	2138	1995	36,308	2570	Pb > Cr > Cd = Zn > Cu > Ni > Co
^c Sauvé et al. (2000)	mean	2884	14,791	4786	4786	16,596	169,824	11,749	Pb > Ni > Co > Zn > Cr = Cu > Cd
^d CETESB (2001)	mean	191	120	4365	537	562	2399	251	Cr > Pb > Ni > Cu > Zn > Cd > Co
^e Allison and Allison (2005)	mean	501	126	6310	316	794	5012	501	Cr > Pb > Ni > Cd = Zn > Cu > Co
	median	794	126	7943	501	1259	12,589	1259	Pb > Cr > Ni = Zn > Cd > Cu > Co
^f USEPA (2019)	–	75	45	****19	35	65	8100	62	Pb > Cd > Ni > Zn > Co > Cu > Cr
				*****1,800,000					Cr > Pb > Cd > Ni > Zn > Co > Cu
Braz et al. (2013a, 2013b)	mean	74	44	52	407	32	851	30	Pb > Cu > Cd > Cr > Co > Ni > Zn
	median	37	34	50	257	24	708	14	Pb > Cu > Cr > Cd > Co > Ni > Zn

^a CrO_4^{2-} ; ^{**}Cr III; ^{***}Cr III and Cr VI; ^{****}Cr VI; ^{*****}Cr total.

^a CSOIL dataset before 2000, in Otte et al. (2001).

^b Revised CSOIL 2000 dataset.

^c Based on total contents ([PTE]_{total}/[PTE]_{dissolved}).

^d Data from the “Report on the establishment of guiding values for soils and groundwater in the State of São Paulo” used up to 2008.

^e Data from extensive literature survey.

^f Data from USEPA generic tables for regional screening levels (RSLs) (<https://www.epa.gov/risk/regional-screening-levels-rsls-generic-tables>).

The Cr(III) species occur in a cationic form of Cr^{3+} , while Cr^{6+} species occur in an anionic form, primarily as CrO_4^{2-} or HCrO_4^- . The cationic form Cr^{3+} is adsorbed to soil more intensively than the CrO_4^{2-} or HCrO_4^- [Cr(VI)] forms. Given the toxic potential of Cr, especially in its hexavalent form, and the difficulty of identifying the species of Cr under different soil conditions, it seems reasonable to consider the potential for higher mobility for the element and to adopt more conservative, lower values for K_d , such as those obtained in this and other studies (VROM, 1994; Buchter et al., 1989; Braz et al., 2013a, 2013b). Anions of the element can have high potential mobility, which is not in accord with high K_d values close to $14,000 \text{ L kg}^{-1}$ (CETESB, 2001). A more restrictive K_d value for Cr(III) is suggested by USEPA (2019). Similarly, the risk due to Ni soil contamination could be underestimated by the use of K_d proposed by CETESB (2001), since the value, 562 L kg^{-1} , is 4.5-fold larger than the median and does not belong to the range of variation found in this study (Table 4).

3.4. Prediction of $\log K_d$

3.4.1. Previous collinearity analysis

The collinearity diagnosis of soil properties detected near dependencies among the variables $\text{Fe}_{\text{Na-DCB}}$, Fe_{OX} , and clay contents ($r \geq 0.8$) (Fig. 6). The clay content was selected as a regressor, while $\text{Fe}_{\text{Na-DCB}}$ and Fe_{OX} highly intercorrelated predictor variables, were suppressed and were not considered in the regression analysis. $\text{Fe}_{\text{Na-DCB}}$ and Fe_{OX} are part of the clay fraction of soils and, therefore, only this fraction is sufficient to represent the effect of clay, $\text{Fe}_{\text{Na-DCB}}$, and Fe_{OX} . Mutual interactions between soil particles are common features in soil and the use of total clay contents seems sufficient to contemplate the effects of different mineralogical components of the soil clay fraction, including phyllosilicates and (oxy)hydroxides. This suggests that no further information is gained when the different components of the soil clay fraction are taken into account.

Collinearity between clay content, OC content, and ECEC was also observed. However, contents of clay and OC may have different effects

on the behavior of PTE in the soil and were considered in the regression model. The high correlation between OC content and ECEC and between clay content and ECEC was also expected, but in weathered soils ECEC represents a particular sorption mechanism, also influenced by pH due to the predominance of variable electrical charges. This means that the ECEC can be changed with pH, even if the contents of clay and OC are the same. Thus, ECEC was also considered in the multiple regression model. The soil attributes considered as independent variables and selected for multiple regression were $\text{pH}_{\text{H}_2\text{O}}$, contents of clay and OC, and ECEC. In the common investigations of contaminated sites, the simplest variables, such as pH and contents of clay and soil organic matter (SOM) are not always measured, while a more detailed assessment of the colloidal fraction of the soil [concentration of (oxy)hydroxides of Fe, Al, and Mn and clay minerals; fractionation of SOM, including DOC], and the chemical speciation of PTE are rarely determined (Yen Le and Hendricks, 2014).

3.4.2. $\log K_d$ best estimates by stepwise linear regression

Data of K_d , $\text{pH}_{\text{H}_2\text{O}}$, clay content, OC content, and ECEC, fitted to a Gaussian distribution after logarithmic transformation, were used in the regression analyses. Log-transformed K_d values are more frequent in the literature and the best default assumption as input for risk assessment models (Carlon et al., 2004; Sheppard et al., 2007; Sheppard, 2011). Eight outlier values detected by the boxplot analysis (Figs. 3 and 5) were not considered in the multiple regression analysis for predicting $\log K_d$: clay content of Arenic Hapludalf-3 (AH-7 soil); Co $\log K_d$ for Arenic Hapludult-3 and Arenic Hapludalf-2 (AH-3 and AH-6 soils); Cr $\log K_d$ for Kandiudalfic Eutrudox (KE), Typic Eutraquox (TH-4), Arenic Hapludult-1 (AH-1), and Typic Argiudoll (TA) soils; Zn $\log K_d$ for Rhodic Eutrudox-2 (RE-2 soil). Backward step-wise regression analyses were used to develop relationships between $\log K_d$ and the soil properties and to obtain partial determination coefficients by progressively excluding independent variables (Table 5).

The first attempts of multiple regressions were made drawing on all the independent variables ($\text{pH}_{\text{H}_2\text{O}}$, clay content, OC content, and ECEC). Theoretically, the use of regression models requires including as many variables as possible, but, from a practical standpoint, K_d estimates should be obtained from a few soil attributes, especially those that are easier to determine. The usefulness of including variables for the models was critically examined for the proportion of the K_d variation that they can explain (Table 6). After eliminating non-significant variables, more simplified models including $\text{pH}_{\text{H}_2\text{O}}$, clay content, and ECEC were obtained (Table 5). Including more than two variables is not expected to provide significant improvement in the R^2 of the predictive equations for $\log K_d$ (Table 5).

Since K_d is a complex function dependent on many soil attributes, it

is often difficult to achieve K_d predictive accuracy for a large number of unrelated soils (Sheppard, 2011). However, the predictive $\log K_d$ equations for all elements of interest were robust, statistically valid, highly significant ($p < 0.001$), and capable of explaining an important part of the K_d variation (R^2 ranging from 0.58 to 0.83) from highly significant variables ($p < 0.001$) (Table 5). The effect of $\text{pH}_{\text{H}_2\text{O}}$, clay content, and ECEC interactions on the $\log K_d$ for Cd, Co, Cr, Cu, Ni, Pb, and Zn was also illustrated by linear regression surfaces in Fig. 7. Correlations between the observed values of $\log K_d$ and those estimated by the regression equations were highly significant, with correlation coefficients varying between 0.76 and 0.91 (Fig. 7).

The distinction between tropical and temperate soils is quite artificial making it difficult to compare the two soil categories (Six et al., 2002). However, an interpretative, critical, and comparative analysis of the $\log K_d$ models (Table 5) with information from the literature on different climatic zones was put forward as a possibility. Each soil attribute considered at first to explain K_d variations was examined in detail.

3.4.2.1. Soil pH. Soil $\text{pH}_{\text{H}_2\text{O}}$ (measured in H_2O suspension; 1:2.5 soil:solution ratio) was the primary predictive attribute, explaining 11–60% of the variation in PTE $\log K_d$ (Table 5). Soil $\text{pH}_{\text{H}_2\text{O}}$ significantly and positively affected $\log K_d$ for almost all elements (Table 5) and some PTE-specific behavior was noted. $\log K_d$ values of the transition metal cations of groups IIB (Cd and Zn) and VIIIB (Co and Ni) were more correlated with soil $\text{pH}_{\text{H}_2\text{O}}$ (48–60%) (Table 6). Soil $\text{pH}_{\text{H}_2\text{O}}$ poorly explained the variation in $\log K_d$ values for Cu (11%) and Pb (34%) (Table 6), which had the highest K_d values (Table 2). On the other hand, soil $\text{pH}_{\text{H}_2\text{O}}$ was not a predictor for Cr $\log K_d$ values (Table 5).

All these interpretations are in agreement with those reported by other authors for tropical, subtropical, and temperate soils (Harter, 1983; Buchter et al., 1989; Janssen et al., 1997; Anderson and Christensen, 1998; Holm et al., 2003; Carlon et al., 2004; Gil-García et al., 2009; Degryse et al., 2009; Braz et al., 2013a, 2013b). The sorption and the $\log K_d$ of cationic PTE are often considered pH-dependent and are generally acknowledged to be directly proportional to the pH, irrespective of the soil type or climate zone (Sposito, 1989; Rieuwerts, 2007). In other studies on soils in Brazil, the soil $\text{pH}_{\text{H}_2\text{O}}$ contribution to explaining the variations in PTE $\log K_d$ was even higher. Braz et al. (2013a, 2013b) observed that $\text{pH}_{\text{H}_2\text{O}}$ explained 66–81% of variation in $\log K_d$ values of transition metal cations and also those in Cu and Pb, in 21 humid equatorial soils from the State of Pará, eastern Amazonia, Brazil.

Clear increases (from 20% to 90%) in the sorption of Zn (Casagrande et al., 2008), Cd (Soares et al., 2009), and Ni (Soares et al., 2011) were reported when the pH of highly weathered tropical Oxisols from the

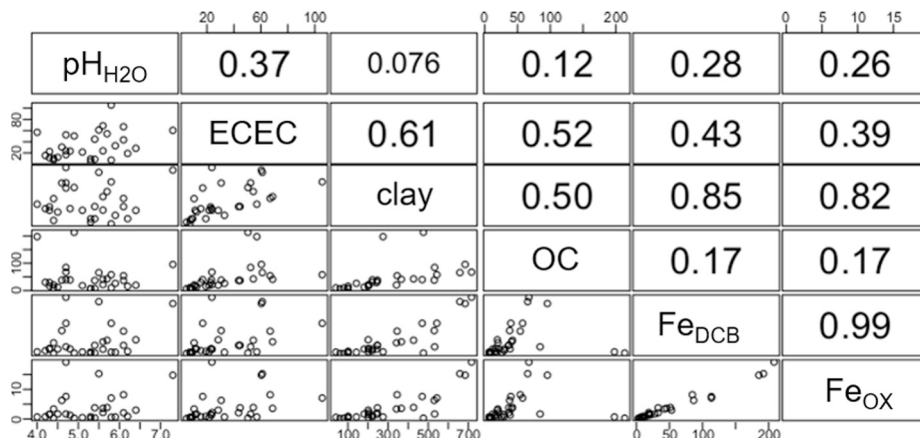


Fig. 6. Collinearity matrix, dispersion graphs, and Pearson's correlation coefficients. The correlation matrix shows the pair-wise correlation among all the explanatory soil variables.

Table 5

Equation parameters for the multiple regression of log-transformed K_d of PTE and selected attributes of soils from the State of São Paulo, southeastern Brazil.

$\log K_d$ ($L \cdot kg^{-1}$)	Intercept (constant)	Soil attributes \pm standard errors				R^2	R_{adj}^2	AIC	n
All independent variables									
$\log K_d Cd =$	$-2.80 \pm 0.85^{***}$	$+0.64 \pm 0.12 \cdot pH_{H2O}^{***}$	$+0.35 \pm 0.40 \cdot clay^{ns}$	$-0.16 \pm 0.41 \cdot OC^{ns}$	$+0.92 \pm 0.47 \cdot ECEC^*$	0.82^{***}	0.79^{***}	54.8	29
$\log K_d Co =$	$-3.83 \pm 0.86^{***}$	$+0.64 \pm 0.12 \cdot pH_{H2O}^{***}$	$+0.69 \pm 0.41 \cdot clay^{ns}$	$-0.30 \pm 0.43 \cdot OC^{ns}$	$+0.88 \pm 0.51 \cdot ECEC^*$	0.83^{***}	0.80^{***}	50.4	27
$\log K_d Cr =$	-2.26 ± 1.45^{ns}	$-0.06 \pm 0.20 \cdot pH_{H2O}^{ns}$	$+2.52 \pm 0.73 \cdot clay^{***}$	$+0.97 \pm 0.88 \cdot OC^{ns}$	$-2.06 \pm 0.96 \cdot ECEC^{**}$	0.63^{***}	0.55^{***}	22.4	25
$\log K_d Cu =$	-0.07 ± 0.65^{ns}	$+0.12 \pm 0.09 \cdot pH_{H2O}^{ns}$	$+0.99 \pm 0.31 \cdot clay^{***}$	$-0.23 \pm 0.31 \cdot OC^{ns}$	$+0.23 \pm 0.36 \cdot ECEC^{ns}$	0.60^{***}	0.53^{***}	70.2	29
$\log K_d Ni =$	$-1.80 \pm 0.66^{**}$	$+0.45 \pm 0.09 \cdot pH_{H2O}^{***}$	$+0.08 \pm 0.32 \cdot clay^{ns}$	$-0.09 \pm 0.32 \cdot OC^{ns}$	$+1.04 \pm 0.36 \cdot ECEC^{**}$	0.83^{***}	0.81^{***}	69.2	29
$\log K_d Pb =$	-0.45 ± 0.73^{ns}	$+0.32 \pm 0.10 \cdot pH_{H2O}^{***}$	$+0.70 \pm 0.35 \cdot clay^*$	$+0.03 \pm 0.35 \cdot OC^{ns}$	$+0.20 \pm 0.40 \cdot ECEC^{ns}$	0.65^{***}	0.60^{***}	63.4	29
$\log K_d Zn =$	$-5.21 \pm 1.45^{***}$	$+0.90 \pm 0.21 \cdot pH_{H2O}^{***}$	$+0.96 \pm 0.55 \cdot clay^*$	$-0.15 \pm 0.59 \cdot OC^{ns}$	$+0.51 \pm 0.72 \cdot ECEC^{ns}$	0.75^{***}	0.71^{***}	37.5	28
After backward stepwise									
$\log K_d Cd =$	$-2.25 \pm 0.46^{***}$	$+0.63 \pm 0.09 \cdot pH_{H2O}^{***}$	$+1.01 \pm 0.21 \cdot ECEC^{***}$			0.81^{***}	0.80^{***}	57.9	29
$\log K_d Co =$	$-2.77 \pm 0.49^{***}$	$+0.62 \pm 0.10 \cdot pH_{H2O}^{***}$	$+1.06 \pm 0.23 \cdot ECEC^{***}$			0.81^{***}	0.79^{***}	51.8	27
$\log K_d Cr =$	$-3.42 \pm 1.12^{**}$	$+3.19 \pm 0.58 \cdot clay^{***}$	$-1.59 \pm 0.51 \cdot ECEC^{**}$			0.58^{***}	0.54^{***}	24.3	25
$\log K_d Cu =$	-0.14 ± 0.52^{ns}	$+0.16 \pm 0.07 \cdot pH_{H2O}^{**}$	$+0.93 \pm 0.17 \cdot clay^{***}$			0.58^{***}	0.55^{***}	73.5	29
$\log K_d Ni =$	$-1.74 \pm 0.35^{***}$	$+0.45 \pm 0.07 \cdot pH_{H2O}^{***}$	$+1.00 \pm 0.16 \cdot ECEC^{***}$			0.83^{***}	0.82^{***}	73.0	29
$\log K_d Pb =$	-0.75 ± 0.59^{ns}	$+0.35 \pm 0.07 \cdot pH_{H2O}^{***}$	$+0.89 \pm 0.20 \cdot clay^{***}$			0.64^{***}	0.62^{***}	66.7	29
$\log K_d Zn =$	$-6.00 \pm 1.05^{***}$	$+1.01 \pm 0.13 \cdot pH_{H2O}^{***}$	$+1.26 \pm 0.31 \cdot clay^{***}$			0.74^{***}	0.72^{***}	40.6	28

Statistical significance: $ns p > 0.1$; $*p < 0.1$; $**p < 0.05$; $***p < 0.01$; $****p < 0.001$.

Stepwise backward procedure without outliers.

pH_{H2O} = in H_2O suspensions (1:2.5 soil:solution ratio).

Clay content by the hydrometer method ($g \cdot kg^{-1}$).

OC = organic carbon content by the Walkley-Black method ($g \cdot kg^{-1}$).

ECEC = effective cation exchange capacity by the summation method (ECEC = $Ca + Mg + K + Al$, in $mmol_c \cdot kg^{-1}$).

AIC = Akaike Information Criterion.

Table 6

Contribution of soil attributes as independent variables (partial R^2) to the final model R^2 of the multiple regression for log-transformed K_d of PTE in soils from the State of São Paulo, southeastern Brazil.

PTE	Partial R^2 (relative importance metrics)				Model R^2
	pH_{H2O}	Clay	OC	ECEC	
All independent variables					
Cd	0.45^{***}	0.06^{ns}	0.06^{ns}	0.25^*	0.82^{***}
Co	0.44^{***}	0.08^{ns}	0.07^{ns}	0.24^*	0.83^{***}
Cr	0.08^{ns}	0.34^{***}	0.12^{ns}	0.09^{**}	0.63^{***}
Cu	0.07^{ns}	0.28^{***}	0.10^{ns}	0.15^{ns}	0.60^{***}
Ni	0.39^{***}	0.06^{ns}	0.08^{ns}	0.30^{***}	0.83^{***}
Pb	0.25^{***}	0.14^{ns}	0.08^{ns}	0.18^{ns}	0.65^{***}
Zn	0.42^{***}	0.06^*	0.05^{ns}	0.21^{ns}	0.75^{***}
After backward stepwise					
Cd	0.49^{***}	–	–	0.32^{***}	0.81^{***}
Co	0.48^{***}	–	–	0.32^{***}	0.81^{***}
Cr	–	0.49^{***}	–	0.09^{***}	0.58^{***}
Cu	0.11^{**}	0.47^{***}	–	–	0.58^{***}
Ni	0.43^{***}	–	–	0.41^{***}	0.83^{***}
Pb	0.34^{***}	0.30^{***}	–	–	0.64^{***}
Zn	0.60^{***}	0.14^{***}	–	–	0.74^{***}

Statistical significance: $ns p > 0.1$; $*p < 0.1$; $**p < 0.05$; $***p < 0.01$; $****p < 0.001$.

Stepwise backward procedure without outliers.

pH_{H2O} = in H_2O suspensions (1:2.5 soil:solution ratio).

Clay content by the hydrometer method ($g \cdot kg^{-1}$).

OC = organic carbon content by the Walkley-Black method ($g \cdot kg^{-1}$).

ECEC = effective cation exchange capacity by the summation method (ECEC = $Ca + Mg + K + Al$, in $mmol_c \cdot kg^{-1}$).

State of São Paulo increased from 4 to 6. For Cu, this sharp increase in sorption was found in these Oxisols when the pH was altered from 4 to 5 (Mouta et al., 2008). The soil pH accounted for 47–88% of the variation in the $\log K_d$ values of Cd, Co, Cu, Ni, and Zn reported in the large database of the International Atomic Energy Agency (IAEA) and of several other reports related to soils in the temperate region (Gil-García et al., 2009). The same high correlation between pH and $\log K_d$ was reported in other major dataset compilations (Sheppard and Thibault, 1990; Sauvé et al., 2000; Carlon et al., 2004) and in more specific situations in temperate soils from Denmark (Anderson and Christensen,

1988; Holm et al., 2003), Netherlands (Janssen et al., 1997), and United States (Buchter et al., 1989). Boekhold et al. (1993) found that increasing pH by 0.5 in the interval between 3.8 and 4.9 doubled Cd sorption in a sandy acidic soil. K_d values for Cd in topsoil horizons of 49 Danish soil samples varied between 70 and 850 $L \cdot kg^{-1}$ at pH 5.3, and from 460 to 2940 $L \cdot kg^{-1}$ at pH 6.7 (Holm et al., 2003). Soil pH is the attribute most commonly cited for its influence on sorption reactions and may be considered the fitting parameter of K_d in several specific situations for metals (Sauvé et al., 2000). At least for Cd, Co, Ni, and Zn, pH seems to be a universal soil parameter for predicting $\log K_d$ values.

Although the pH_{H2O} was not collinear with another soil attribute (Fig. 6), it is difficult to dissociate its influence on other soil attributes and the combined effect on the sorption of PTE (Sauvé et al., 2000). The pH may also correlate strongly with soil components such as phyllosilicates, (oxy)hydroxides, or organic matter and thus mask their clear contribution to PTE sorption (Holm et al., 2003). Its strong effect on PTE sorption is a function of the changes it causes in various parameters of the solid and liquid phases of the soil. For this reason, the pH effect is found neither in less weathered soils of the temperate zone nor in highly weathered tropical soils.

Regardless of edaphoclimatic conditions, soil pH regulates the chemical speciation of the elements present in the soil solution. Increased element sorption with increasing pH is strongly attributed to a free PTE pool (PTE^{2+}), to changes in the hydrolysis state of ions [e.g. $PTEOH^+$, $PTE(OH)_2^0$, $PTE(OH)_3^+$ (Yu, 1997; Sposito, 1989)], to formation of inorganic ion pairs in solution [e.g. $PTEHCO_3^-$, $PTECO_3^0$, $PTE(CO_3)_2^{2-}$, $PTENO_3^-$, $PTECl^+$, $PTEO_4^0$, etc. (Sauvé et al., 2000)], and to complexes with DOM (Yin et al., 2002; Gmach et al., 2019; Schneider et al., 2019). The pH dependence of sorption reactions of cationic PTE is due, in part, to the preferential sorption of the hydrolyzed species in comparison to the free ions (Harter, 1983).

The proportion of hydrolyzed species increases with pH and the degree by which the cationic PTE are hydrolyzed is a specific, intrinsic characteristic of each chemical element. Hydrolyzed species predominate in the solution of soils with pH values close to or above neutrality, and are more common in temperate regions. The energy barrier that must be overcome when hydrolyzed ions approach the surface of soil particles is decreased and sorption is favored (Yu, 1997; Casagrande et al., 2008). Our PTE K_d (Table 2) did not discriminate the ionic species involved in the sorption process, and this is a limitation of the K_d index

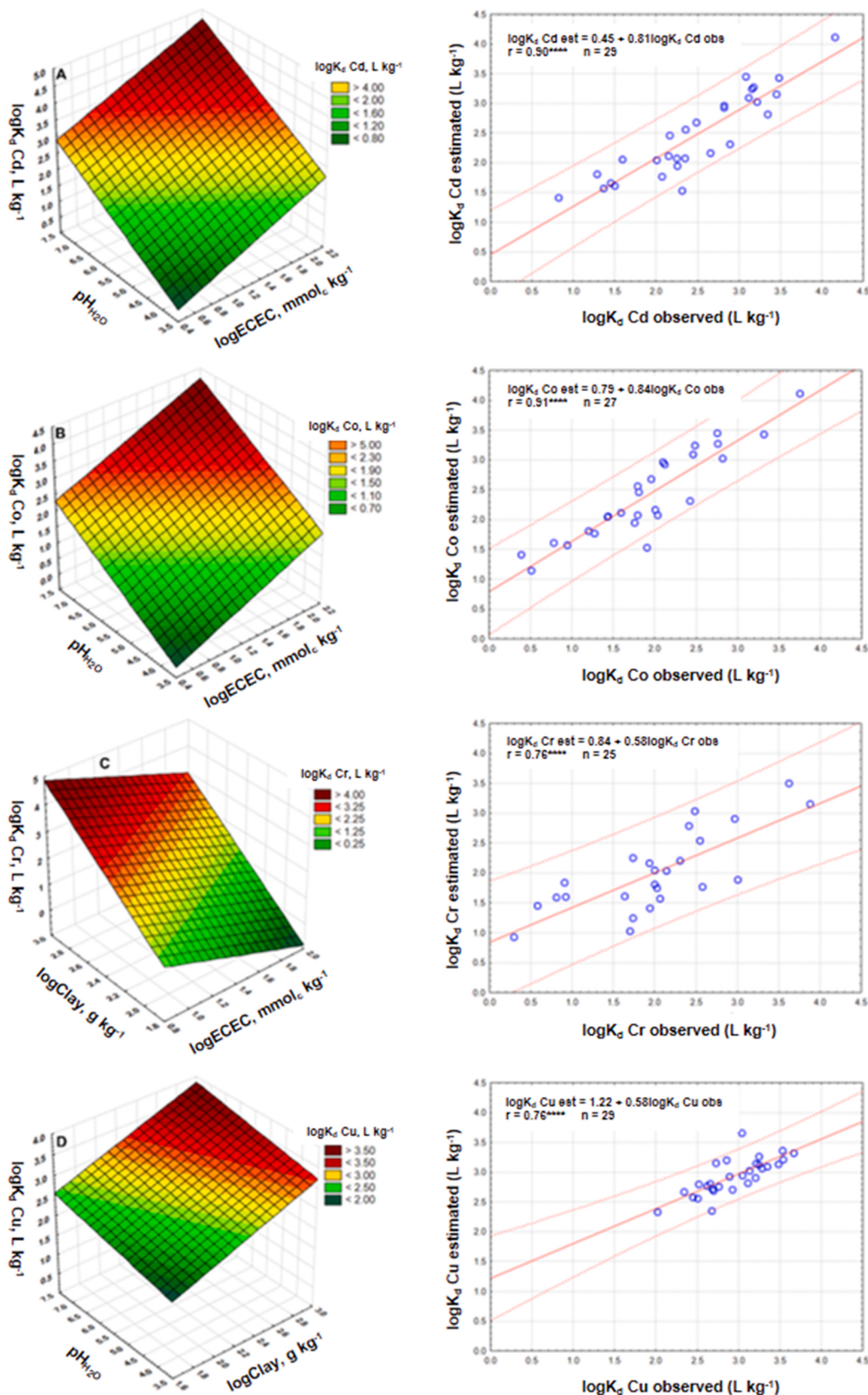


Fig. 7. Regression response surface (RRS) and the extent of the linear fit of $\log K_d$ of Cd, Co, Cr, Cu, Ni, Pb, and Zn (A, B, C, D, E, F, and G, respectively) as a function of soil attributes selected after backward stepwise analysis. Additional graphs show the correlation between experimental values versus estimated values by the regression equations; dashed lines indicate a 95% prediction interval; pH_{H_2O} = in H_2O suspensions (1:2.5 soil:solution ratio); ECEC = effective cation exchange capacity by the summation method ($ECEC = Ca + Mg + K + Al$, in $\text{mmol}_c \text{ kg}^{-1}$); clay content by the densimeter method (g kg^{-1}).

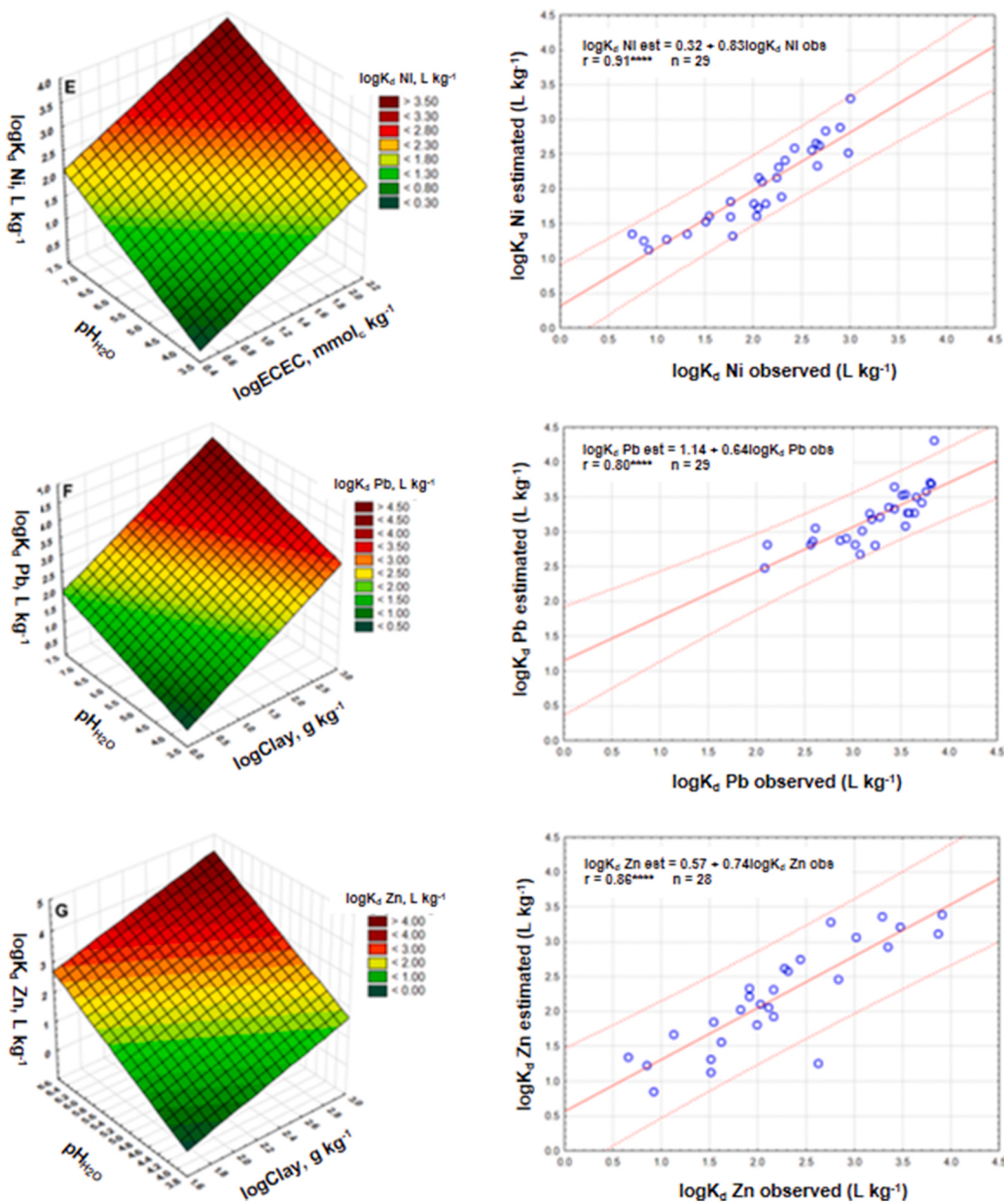


Fig. 7. (continued).

widely reported in the literature.

An important aspect related to speciation may explain the results of $\text{Cr } K_d$. The variation in $\log K_d$ values for Cr was not explained by pH, similar to that observed in American (Buchter et al., 1989) and Dutch soils (Janssen et al., 1997), as well as in the large soil database used by Sheppard (2011). The absence of a pH effect of Dutch soils on K_d was attributed to the anionic speciation of Cr (Janssen et al., 1997). Chromium persists in the environment as either Cr(III) or Cr(VI) as it is a redox reactive metal. Its K_d can follow the same pH dependence as other cationic metals when in a reduced form of Cr(III). Generally, sorption of Cr decreases with increasing pH, while the rate of reduction in Cr(VI) increases with decreasing pH (Fendorf, 1995). Therefore, the anionic character of the Cr(VI), such as HCrO_4^- , makes sure that pH dependence is opposite to that of the cationic metals.

In typical acidic and weathered tropical soils, the association between cation sorption and pH is due partly to the competition of H^+ and Al^{3+} ions for sorption sites at low pH, resulting in decreased cationic PTE sorption. However, as pH went up, the concentrations of OH^- increased, which resulted in the increasing competition between CrO_4^{2-} and OH^-

and the decrease in CrO_4^{2-} sorption (Shi et al., 2020). Speciation is an additional factor affecting Cr K_d and this is a key aspect of Cr behaviour often neglected in the literature. Normally, data from experiments performed with Cr(III) and Cr(VI) means that there is no statistical correlation between $\log K_d$ and pH (Gil-García et al., 2009; Galán et al., 2019).

Predicted $\log K_d$ values become more accurate when, in addition to pH, other soil attributes are also included in the regression equations. Although this significantly improves the R^2 for all the PTE studied, the relative amelioration was metal-specific (marginal for Cr and Zn and between 30 and 47% for the other PTE) (Tables 5 and 6). The effect of pH on other soil attributes is discussed below.

3.4.2.2. Soil clay contents. The mineralogical composition of the fine-grained soil fraction varies considerably according to climate zone, mainly due to the intensity of weathering (Kämpf et al., 2019). Typically, in an inorganic colloidal system of highly weathered tropical soils from the humid zone, the 1:1 layer-type phyllosilicates (mainly kaolinite) and Fe and Al (oxy)hydroxides (mainly hematite, goethite,

and gibbsite) are predominant (Schaefer et al., 2008; Alleoni et al., 2009). In temperate soils, a fair proportion of the clay fraction is usually composed of 2:1 layer-type silicate minerals (illite, smectite, vermiculite, and montmorillonite) (Azevedo and Vidal-Torrado, 2019). The mineralogical dominance and physicochemical characteristics of secondary minerals affect the soil's ability in terms of sorption processes of PTE (Six et al., 2002; Bradl, 2004; Shaheen et al., 2013).

In addition to soil pH, total clay content introduces distinguished improvements in the estimates of K_d values for Cu, Cr, Pb, and Zn through alternative simplified equations (Tables 5 and 6). The combined action of these factors was different for each element, and a metal-specific behaviour was again observed (Tables 5 and 6, and Fig. 7). Soil pH tends to influence differently the colloidal charge density of soils from tropical and temperate zones. In tropical regions, soil pH strongly affects the sign and magnitude of electrical charges on amphoteric, variable-charged colloid surfaces, due to the variation in the intensity of deprotonation of the electrically charged surface of Fe and Al (oxy)hydroxides, organic matter, and 1:1 layer-type phyllosilicate edges (Six et al., 2002; Alleoni et al., 2009). Thus, PTE tend to be sorbed at different pH values in weathered soils since sorption occurs on surfaces having a charge density strongly dependent on pH.

Considering the clay content and the levels of pedogenic crystalline and amorphous Fe (oxy)hydroxides as collinear variables (Fig. 6) was a wise decision to simplify the regression models. For a practice-based approach, such as in the generating of estimated K_d values to use in risk assessment models, more easily determined variables and routinely measured soil properties such as total clay content are preferred by modellers and end-users (Janssen et al., 1997).

Many authors have shown the importance of including different components of the clay fraction in the regression models (Takata et al., 2014; González-Costa et al., 2017). Janssen et al. (1997) studied variation in As, Cd, Cr, Cu, Pb, and Zn field-based K_d values in soil samples collected from 20 sites in the Netherlands and by taking into consideration the total clay content, the isolated effect of amorphous phase of Fe (oxy)hydroxide on the partitioning of As, Cu, and Pb was also detected. Gibbsite was the most important component for the sorption of Cd and Zn, while clay minerals (kaolinite, vermiculite, and chlorite) were better able than Fe, Al, and Mn (hydr)oxides to adsorb Cr, Cu, and Pb in acidic soils from Galicia, NW Spain (González-Costa et al., 2017). The regression models obtained by Braz et al. (2013a) discriminated the isolated involvement of the different forms of Fe and Al (oxy)hydroxides in a set of Amazonian soils in the definition of K_d values for Co, Cu, Ni, Pb, and Zn.

Braz et al. (2013a, 2013b) used soils similar to those used in this study, from the point of view of classification (Oxisols, Ultisols, Alfisols, Entisols, etc.). However, there is a very clear distinction between Brazilian climate units where soils are inserted, which implies a distinct influence of precipitation, temperature, and vegetation cover in the rate of chemical reactions of soil weathering. Although 90% of the country is within the tropical zone, the climate of Brazil varies considerably (equatorial, semi-arid, tropical, highland tropical, and subtropical) from the mostly tropical North (the equator traverses the mouth of the Amazon) to temperate zones below the Tropic of Capricorn ($23^{\circ}27' S$ latitude). Braz et al. (2013a, 2013b) studied Brazilian soils in the humid equatorial zone (state of Pará, eastern Amazon, Brazil), characterized by an abundant and regular average rainfall of 2500 mm yr^{-1} , average annual temperatures of 25°C ($\pm 3^{\circ}\text{C}$), exuberant vegetation, and, consequently, intense weathering rates. The characteristic mineral association is Fe and Al (oxy)hydroxides, due to the predominance of the alitization/ferralsilization process. For our study, soils were collected in the sub-humid tropical zone (State of São Paulo, southeastern Brazil) (Table 1), with hot and humid summers, and dry and cold winters. The average annual temperature is 20°C ($\pm 7^{\circ}\text{C}$) and the average rainfall in excess of 500 mm yr^{-1} , concentrated in the summer. This is a more moderate weathering environment, in which monossialitization is the dominant process and the main mineral species in the clay fraction are

1:1 phyllosilicates (mainly kaolinite), with important and varied occurrence of Fe and Al (oxy)hydroxides (Schaefer et al., 2008; Kämpf et al., 2019). On the other hand, even with the recognized importance of the clay fraction on the behavior of metals in soils, some studies in the temperate zone (United Kingdom, France, Netherlands, Denmark, and United States) did not include the clay fraction as a predictive factor of K_d values (Gerritse and Van Driel, 1984; Sheppard and Thibault, 1990; Anderson and Christensen, 1988; Janssen et al., 1997; Sauvé et al., 2000; Tipping et al., 2003; Holm et al., 2003; Gil-García et al., 2009).

The qualitative aspect of the clay fraction would allow for greater understanding of the effect of the typical mineral composition of tropical (dry or humid) or temperate regions on the K_d values, including possible arguments about sorption mechanisms (inner- or outer-sphere) (Peng et al., 2018; Qu et al., 2019). Alfisols and Entisols presented 180 g kg^{-1} as mean clay content (Table 1). However, this set of soils, except for Typic Quartzipsamment soil, did not show such low values for K_d (Table 2), due to the presence of 2:1 layer-type phyllosilicates (illite and hydroxy-interlayered vermiculite) (Table 1 and Fig. 2), the predominant qualitative aspect of the soil clay fraction.

In humid tropical conditions the occurrence of 2:1 layer-type phyllosilicates is not a typical feature and is observed under peculiar conditions only, as an accessory of secondary minerals in soils (Azevedo and Vidal-Torrado, 2019) such as the Arenic Hapludalfs (AH-5, AH-6, and AH-7), Typic Hapludalfs (TH-6 and TH-7), Lithic Udtortent (LU), and Typic Ustorthent (TU) soils (Table 1). Oxisols and Ultisols presented mean clay content of 350 g kg^{-1} and high K_d values were observed for these sets of soils. Kaolinite, 1:1 layer-type phyllosilicate with recognized low activity compared to 2:1 layer-type phyllosilicates, was predominant in the clay fraction of these soils (Table 1). The significantly lower CEC of the dominant 1:1 clays leads to the expectation that the clay fraction of many tropical soils will be less important in retaining cationic PTE than that of temperate soils. However, high levels of Fe and Al (oxy)hydroxides can give the soil greater capacity for specific sorption of elements (Spark et al., 1995; Rieuwerts, 2007). This point to a unique effect of the clay fraction related to inherent aspects that, in tropical soils, goes beyond the cation exchange capacity (CEC).

3.4.2.3. Effective cation exchange capacity (ECEC) and sorption mechanisms. Since various PTE occur as cationic species, the significant correlation between ECEC and K_d values for Cd, Co, Cu, Ni, Pb, and Zn was expected. ECEC explained 32–41% of the variation in the log K_d values of Cd, Co, and Ni (Tables 5 and 6). Retention of PTE ions by charged surfaces of soil components is broadly grouped into non-specific (outer-sphere, by ion exchange) and specific (inner-sphere, by surface complexation) mechanisms (Bolan et al., 2014). The CEC is responsible for retaining positively charged ions by electrostatic mechanisms (outer-sphere) and is a soil attribute directly dependent on the clay fraction and the organic matter contents (Fig. 6). The OC content may account for 50–95% of the CEC of humid tropical soils (Soares and Alleoni, 2008).

In soils from temperate regions, the 2:1 layer-type clay minerals manifest high ECEC due to the permanent nature of their surface charges, which are not affected by changes in soil solution parameters. The relatively weak metal binding of 2:1 layer-type phyllosilicates by CEC, compared to binding to Fe, Al, and Mn (oxy)hydroxides, is an important reason that can explain the absence of clay as an important sorption phase in temperate soils (Janssen et al., 1997). Thus, simple ion exchange phenomena are a more typical occurrence of minerals contained in the clay fraction of temperate soils and the influence of the clay fraction may be implicit in ECEC or vice versa.

Extreme changes in the sorption of PTE may occur within the pH range of variation observed for the soils (Table 1). The Fe and Al (oxy) hydroxides play an especially important role in PTE sorption and K_d in soils through specific sorption mechanism, a type of inner-sphere complexation (Spark et al., 1995). In this context, ion exchange

reactions may not be the primary mechanism of sorption of PTE in tropical soils. Kalbasi et al. (1978) estimated that 60–90% of the sorption of Zn by Fe and Al (oxy)hydroxides was accounted for by specific sorption mechanisms, while 10–40% was due to non-specific electrostatic mechanisms. These are a key feature that differentiate the participation of the clay fraction in K_d predictions for tropical soils.

There was no direct effect of ECEC on Cu, Pb, and Zn K_d (Table 5) which supports the notion of a low contribution of non-specific sorption as a retention mechanism, probably due to a higher affinity with (oxy) hydroxides in tropical soils. In the equation obtained for variation in the $\log K_d$ values for Cr, Cu, Pb, and Zn, only clay content and pH_{H2O} were significant parameters (Tables 5 and 6). This point to an exclusive effect of the clay fraction, which cannot be related exclusively to CEC. Therefore, the sorption of PTE (at least Cr, Cu, Pb, and Zn – Table 5) in soils with appreciable amounts of Fe and Al (oxy)hydroxides must be associated with other mechanisms that do not involve simple ionic or electrostatic bonds.

A number of authors have reported that sorption of Cd, Cu, Ni, Pb, and Zn was dependent on the ECEC of tropical soils (Alleoni et al., 2005; Linhares et al., 2009; Braz et al., 2013a, 2013b). Matos et al. (1996) found that more than 60% of the retention of Cd in the topsoil layer of an Oxisol was associated with the exchangeable fraction of the soil, which highlights the greater contribution of lower-energy bonds. Camargo et al. (1989) found that maximum sorption of Ni in topsoil samples of Brazilian Oxisols was correlated with CEC, and considered specific sorption mechanisms of the element to be unimportant. On the other hand, in Brazilian Oxisols, Alfisols, and Ultisols, maximum sorption of Zn was not caused by the CEC effect because the high contents of (oxy) hydroxides of the clay fraction may promote the specific sorption of Zn (Cunha et al., 1994). Casagrande et al. (2008) identified specific sorption mechanisms for Zn in extremely weathered Oxisols only at pH values below 5.0. According to Soares et al. (2009), specific sorption of Ni by Oxisols predominates at pH values between 3 and 5, while at pH values above 5 Ni was electrostatically adsorbed. The direct and isolated effect of the clay fraction on Pb sorption was observed in tropical soils. Its low mobility was attributed to its strong interaction with kaolinite and/or the soil oxide fraction, mostly mediated by specific sorption mechanisms (Matos et al., 1996; Araújo et al., 2002). High $\log K_d$ values for Cr can be found in soils with a high clay content, across a wide range of pH. Although Cr(VI) is therefore not appreciably retained by the negative charged colloids in soils, it is sorbed on many (oxy)hydroxides. Bradl (2004) has noted that Cr^{3+} is rapidly and specifically adsorbed by Fe and Al (oxy)hydroxides and clay minerals. Alcântara and Camargo (2001) raised the possibility that the high sorption of Cr by Fe and Al (oxy)hydroxides disguises the effect of organic matter in retaining the element.

Statistical models relating K_d to soil properties are empirical approaches but their mathematical form can be explained by soil chemical reactions (Degryse et al., 2009). However, some information on sorption mechanisms was obtained by the types of isotherms (Table 2). H-type curves, whose initial slope is associated with high affinity and inner-sphere surface complexation, were adjusted to describe the sorption of Cu and Pb. Concomitantly, these adjustments resulted in the highest K_d values (Table 2). Metals are specifically sorbed in the preferential order $Cd < Zn < Cu < Pb$ (Alloway, 2013), as noted in this study and by Braz et al. (2013a, 2013b), which are typical K_d databases for Brazilian soils.

3.4.2.4. Soil organic carbon (SOC) contents. The SOC had little influence on the PTE $\log K_d$. Contributions of SOC to the explanation of the $\log K_d$ values did not exceed 12% and, in all regression models, SOC was not a statistically significant predictor (Tables 5 and 6). In addition, coefficients of SOC in the $\log K_d$ Cd, Co, Cu, Ni, and Zn predictions equations were negative (Table 5). After backward regression analysis, SOC was excluded from the models and did not cause a reduction in the

determination coefficients or in the statistical significance of the models (Tables 5 and 6). Among the divalent first row transition elements, Cu has the greatest affinity for OC and is preferentially adsorbed before other metals by SOC (Silveira et al., 2002; Silveira and Alleoni, 2003; Mouta et al., 2008) especially at low concentrations. The contribution of SOC was more important to Cu, which explained 12% of the variation in $\log K_d$ values but with a non-significant coefficient ($p > 0.1$).

There is a vast and controversial field of literature about the influence of SOC on the behavior of PTE in soils (Wiatrowska and Komisarek, 2019). It is difficult to distinguish the effects of SOC since its composition tends to vary across soils. Temperate and tropical soils differ according to the conditions of production, accumulation, and degradation of organic matter (biomass plant production, soil microbial diversity and activity, climate, parent material) (Six et al., 2002). In addition, SOC may act both in the solid phase of the soil, as a source of pH dependent changes, and in the soil solution by the formation of organic PTE complexes which affect its sorption.

An increase in SOC increased the K_d values for several radiologically and chemically toxic elements in Canadian soils (Sheppard and Thibault, 1990). This trend was not restricted to soil from specific areas, because it was the same for studies with large databases for soils from France, United Kingdom, and Netherlands (Gerritsen and Van Driel, 1984; Sauvé et al., 2000). For Cd, this correlation was also clearly observed in soils from the United States (Lee et al., 1996), Canada (Sheppard and Thibault, 1990), and Denmark (Anderson and Christensen, 1988; Holm et al., 2003). On the basis of Sauvé et al. (2000) and Janssen et al. (1997) datasets, $\log OC$ in soils are not significant predictors of Pb $\log K_d$. However, $\log OC$ was highly positively correlated to Pb $\log K_d$ in the Gerritsen and Van Driel (1984) dataset. According to Braz et al. (2013a, 2013b), organic matter correlated only with K_d values for Cd in tropical soils of the Amazon region.

More often, dissolved organic carbon (DOC), a more specific part of SOC, is a component of most regression models that explain variations in K_d for PTE in temperate soils (Temminghoff et al., 1997; Degryse et al., 2009; Liu et al., 2018; Schneider et al., 2019). SOC and DOC are greatly influenced by changes in soil pH, but differently in tropical and temperate regions. Since the concentration of DOC tends to increase with increasing pH, this is not a typical situation for tropical acid soils. The functional groups also ionize increasingly as pH rises and organo-metal complexes thus become increasingly stable with the elevation of soil pH close to neutrality, a typical situation that may explain the greater effect of organic matter on the dynamics of metals in temperate soils (Stevenson, 1994).

Soluble organic acids are important components of the soil DOC, which have carboxylic and phenolic functional groups that increase PTE sorption (Gmach et al., 2019). Temminghoff et al. (1997) reported that, at pH 6.6, >99% of Cu in soil solution was predicted by models to be bound to DOC, decreasing to 30% at pH 3.9. Conversely, cationic metal mobility has been observed to increase with rising pH due to the formation of metal complexes with DOC. Thus, DOC does not always favor PTE sorption by the soil (Janssen et al., 1997; Sauvé et al., 2000; Yin et al., 2002; Holm et al., 2003; Carlon et al., 2004; Mouta et al., 2008; Degryse et al., 2009; Gil-García et al., 2009). SOC was an insignificant factor in solid-solution distribution of Cu in 17 major agricultural soil types in China, but the active fraction of DOC was important in improving model estimates (Zhang et al., 2018).

The DOC is a subject still little explored by the science of tropical soils, but it is known that under more typical condition of acid soils, the solubility of DOC is diminished by the high degree of protonation resulting from low pH (Zhang et al., 2018). In tropical soils, SOC is an important variable charge soil component. The active components in metal binding by organic matter are the negatively-charged functional groups such as phenol, carboxyl, and amino groups (Stevenson, 1994). As the pH increases, the degree of negative charges increases due to protonation or dissociation of H^+ from functional groups. Since its point of zero charge (PZC) is low, SOM is negatively charged at pH values

greater than 3.0, with a high sorptive capacity at pH levels of 5 and above (Alloway, 2013).

Another aspect associated with the action of SOC in tropical soils is the formation of organomineral complexes (Kaiser and Guggenberger, 2003). The mineralogical composition of the clay fraction is the primary factor for organomineral complex, since phyllosilicates may not have the same linkage potential with SOC as (oxy)hydroxides have (Jardine et al., 1989). The proportion of amphoteric sites in the surface of Fe and Al (oxy)hydroxides is larger than in the surface of phyllosilicates, increasing the probability of this linkage occurring between minerals with organic surfaces, leading to formation of more stable organo-oxicidic complexes. In a previous study on the same set of soils used in this study (Table 1), Soares and Alleoni (2008) reported that SOC were strongly associated with clay ($r = 0.90$; $p < 0.01$) and crystalline Fe (oxy)hydroxides contents ($r = 0.86$; $p < 0.01$). Recent study of Rasmussen et al. (2018) showed that Fe and Al (oxy)hydroxides emerged as better predictors of SOM stabilization and formation of organomineral complexes with increasing moisture availability and soil acidity.

The fine soil fraction, composed of phyllosilicates and crystalline and amorphous Fe and Al (oxy)hydroxides contribute to the preservation of organic carbon in soil (Müller and Höper, 2004; Wiseman and Püttman, 2006). It is suggested that a portion of the Fe and Al (oxy)hydroxides, as well as other possible sorption sites, are generally coated or occluded by organic matter. Studies have found that soil organic matter could adsorb onto the surface of soil minerals, blocking some of the binding sites of minerals (Qu et al., 2019; Shi et al., 2020).

4. Conclusions

The use of generic K_d values might lead to a serious misinterpretation of area contamination level and gross error if used to predict negative impacts on environmental resources and public health. Modelers and end-users can choose to use our median K_d values (Table 2) for any soil or to apply our regression models using simple soil attributes (Table 5). The first approach was based on the examination of the best measure of the central tendency of the data and then unique K_d values for each PTE were compared with the default K_d of several international databases. As another option, semi-mechanistic regression models for estimating K_d values using soil attributes of easy determination were also proposed. Our regression equations were necessarily simple, highly significant ($p < 0.001$), and PTE-specific. Proportions of 58–83% of the variation in K_d values were explained using linear regressions that included $\text{pH}_{\text{H}_2\text{O}}$, effective cation exchange capacity (ECEC), and clay contents. Soil pH was the primary predictive attribute, explaining 11–60% of the PTE $\log K_d$ variation. The behavior of transition metal cations of groups IIB (Cd and Zn) and VIIIB (Co and Ni), whose K_d were more correlated with soil pH (48–60%), tends to be more worrying because the soil pH, unlike other soil attributes such as clay content, can undergo natural (though mainly induced) major changes in a short time (Zhang et al., 2019), and result in drastic variations in K_d values. The sorption of PTE can minimize their passage into surface and groundwater, but at the same time it creates the possibility that the alteration of soil conditions (mainly soil pH) may result in the release of the accumulated load into the soil solution, thereby opening up an easy passage for PTE to enter the food chain.

Though the approach is more accurate, regression equations has not been used frequently for practical purposes. The applicability of regression models is also usually limited to the range of conditions and soils used to derive these relationships, but our set of soils showed a wide range of chemical, physical, and mineralogical attributes. We encourage the intensification resulting from using K_d values from multiple regression algorithms because it is a more robust and safe method that may provide faster, lower-cost alternatives to laboratory-based methods. Additionally, this method decreases the uncertainty in estimation and removes the need for new K_d values for each environmental condition.

Site specific modifications of K_d values to input into environmental

fate models should minimally correct using an empirical approach similar to the linear regression described in Table 5. The application of the regression model to estimate K_d instead of using conservative assumptions, i.e. the lowest K_d value in the range of variability for the specific element as reported in the literature for fate and transport modelling risk assessment procedures, may reduce the risk of estimation by several orders of magnitude.

The K_d values proposed here will also help regulatory agencies to better review soil standards and regulate RGV to protect environmental and public health. In the specific case of CETESB, these K_d values may be more appropriate for insertion in the current spreadsheet used to calculate the intervention values, for the following reasons: K_d values were obtained via laboratory batch type sorption experiments under the partitioning theory; use of a larger and more representative set of soils than those previously used by CETESB (2001), covering a wide range of soil attributes; and determining the contents of the elements of interest by high-tech instrumental analysis technique (HR-ICPMS).

Although an important amount of data has been added to the K_d database for humid tropical soils, there are still evident gaps for a large number of PTE considered by CETESB as priority contaminants. We advise that K_d values for other high-priority PTE should be obtained under the same conditions as those in this study. In the stage of refined improvements in K_d values, studies of PTE chemical speciation (K_d for the free ion, the complex, the ligands, and the total metal), fractionation of soil organic matter (solid and liquid phases), competitive-PTE sorption systems, and modeling of the sorption phenomenon have been mentioned (Yin et al., 2002; Degryse et al., 2009; Zhang et al., 2018; Qu et al., 2019; Schneider et al., 2019).

Finally, since most K_d databases are developed for temperate regions, this study participates in the expansion of the few K_d databases developed for soils from humid tropical regions. We also observed that our K_d values and regression models, obtained for the sub-humid tropical zone (State of São Paulo, southeastern Brazil) were different from those obtained in the equatorial zone (State of Pará, eastern Amazon, Brazil) (Braz et al., 2013a; 2013b). These differences showed that K_d values might not be completely suitable for widespread use in territories of large extensions, where the variability of climatic types is observed. Thus, we draw attention to the need to obtain regional K_d values whenever possible.

Credit author statement

Marcio Roberto Soares: Conceptualization, Methodology, Validation, Formal Analysis, Investigation, Data Curation, Writing – Original Draft, Writing – Review & Editing, Visualization. Jorge Eduardo de Souza Sarkis: Formal Analysis, Methodology. Luis Reynaldo Ferracciú Alleoni: Conceptualization, Data Curation, Funding acquisition, Project administration, Supervision, Writing – Review & Editing.

Declaration of competing interest

The authors declare that they have no known competing financial interests or personal relationships that could have appeared to influence the work reported in this paper.

Acknowledgements

This work was supported by the São Paulo Research Foundation (FAPESP), Brazil [grant numbers 02/00003-5 and 03/00192-5].

References

- Abrahams, P.W., 2002. Soils: their implications to human health. *Sci. Total Environ.* 291, 1–32. [https://doi.org/10.1016/S0048-9697\(01\)01102-0](https://doi.org/10.1016/S0048-9697(01)01102-0).
- Alcântara, M.A.K., Camargo, O.A., 2001. Isotermas de adsorção de Freundlich para crômio (III) em Latossolos. *Sci. Agric.* 58, 567–572. <https://doi.org/10.1590/S0103-90162001000300020>.

- Alleoni, L.R.F., Iglesias, C.S.M., Mello, S., Camargo, O.A., Casagrande, J.C., Lavorenti, N.A., 2005. Atributos do solo relacionados à adsorção de cádmio e cobre em solos tropicais. *Acta Sci. Agron.* 27, 729–737. <https://doi.org/10.4025/actasciagron.v27i4.1348>.
- Alleoni, L.R.F., Peixoto, R.T.G.P., Azevedo, A.C., Melo, L.C.A., 2009. Components of surface charge in tropical soils with contrasting mineralogies. *Soil Sci.* 174, 629–638. <https://doi.org/10.1097/SS.0b013e3181c17a93>.
- Allison, J.D., Allison, T.L., 2005. Partition coefficients for metals in surface water, soil, and waste (EPA/600/R-05/074). https://cfpub.epa.gov/si/si_public_record_report.cfm?Lab=NERL&dirEntryId=135783. (Accessed 15 March 2020).
- Alloway, B.J., 2013. Heavy Metals in Soils: Trace Metals and Metalloids in Soils and Their Bioavailability, third ed. Springer, London.
- Anderson, P.R., Christensen, T.H., 1988. Distribution coefficients of Cd, Co, Ni and Zn in soils. *J. Soil Sci.* 39, 15–22. <https://doi.org/10.1111/j.1365-2389.1988.tb01190.x>.
- Aratijo, W.S., Amaral-Sobrinho, N.M.B., Mazur, N., Gomes, P.C., 2002. Relação entre adsorção de metais pesados e atributos químicos e físicos de classes de solos do Brasil. *Rev. Bras. Cienc. Solo* 26, 17–27. <https://doi.org/10.1590/S0100-06832002000100003>.
- Assad, E.D., Pinto, H.S., Martins, S.C., Gropp, J.D., Salgado, P.R., Evangelista, B., Vasconcelos, E., Sano, E.E., Pavão, E., Luna, R., Camargo, P.B., Martinelli, L.A., 2013. Changes in soil carbon stocks in Brazil due to land use: paired site comparisons and a regional pasture soil survey. *Biogeosciences* 10, 6141–6160. <https://doi.org/10.5194/bg-10-6141-2013>.
- ATSDR - Agency for Toxic Substances and Disease Registry, 2019. The ATSDR 2019 substance priority list. <https://www.atsdr.cdc.gov/spl/index.html#2019spl>. (Accessed 10 October 2020).
- Augustsson, A., Uddh Söderberg, T., Jarsjö, J., Åström, M., Destouni, G., 2016. The risk of overestimating the risk-metal leaching to groundwater near contaminated glass waste deposits and exposure via drinking water. *Sci. Total Environ.* 566–567, 1420–1431. <https://doi.org/10.1016/j.scitotenv.2016.06.003>.
- Azevedo, A.C., Vidal-Torrado, P., 2019. Esmectita, vermiculita, minerais com hidroxi entrecamadas e clorita. In: Melo, V.F., Alleoni, L.R.F. (Eds.), Química e Mineralogia do Solo. Sociedade Brasileira de Ciencia do Solo, Vicosia, pp. 381–426.
- Bell, J., Bates, T.H., 1988. Distribution coefficients of radionuclides between soils and groundwaters and their dependence on various test parameters. *Sci. Total Environ.* 69, 979–986. [https://doi.org/10.1016/0048-9697\(88\)90349-X](https://doi.org/10.1016/0048-9697(88)90349-X).
- Bernoux, M.B., Carvalho, M.D.S., Volkoff, B., Cerri, C.C., 2002. Brazil's soil carbon stocks. *Soil Sci. Soc. Am. J.* 66, 888–896. <https://doi.org/10.2136/sssaj2002.0888>.
- Bocking, G.J.M., van de Plassche, E.J., Struijs, J., Canton, J.H., 1992. Soil-water partition coefficients for some trace metals (RIVM Report No. 679101003). <http://www.rivm.nl/bibliotheek/rapporten/679101003.pdf>. (Accessed 4 September 2020).
- Boekhold, A.E., Temminghoff, E.J.M., Van der Zee, S.E.A.T.M., 1993. Influence of electrolyte composition and pH on cadmium sorption by an acid sandy soil. *Eur. J. Soil Sci.* 44, 85–96. <https://doi.org/10.1111/j.1365-2389.1993.tb00436.x>.
- Bolan, N., Kunhikrishnan, A., Thangarajan, R., Kumpiene, J., Park, J., Makino, T., Kirkham, M.B., Scheckel, K., 2014. Remediation of heavy metal(loid)s contaminated soils - to mobilize or to immobilize? *J. Hazard Mater.* 266, 141–166. <https://doi.org/10.1016/j.jhazmat.2013.12.018>.
- Bradl, H.B., 2004. Adsorption of heavy metal ions on soils and soil constituents. *J. Colloid Interface Sci.* 277, 1–18. <https://doi.org/10.1016/j.jcis.2004.04.005>.
- Brand, E., Otte, P.F., Lijzen, J.P.A., 2007. CSOIL 2000 an exposure model for human risk assessment of soil contamination: a model description (RIVM Report No. 711701054). <http://www.rivm.nl/bibliotheek/rapporten/711701054.html>. (Accessed 21 July 2020).
- Braz, A.M.S., Fernandes, A.R., Ferreira, J.R., Alleoni, L.R.F., 2013a. Distribution coefficients of potentially toxic elements in soils from the eastern Amazon. *Environ. Sci. Pollut. Res.* 20, 7231–7242. <https://doi.org/10.1007/s11356-013-1723-9>.
- Braz, A.M.S., Fernandes, A.R., Ferreira, J.R., Alleoni, L.R.F., 2013b. Prediction of the distribution coefficients of metals in Amazonian soils. *Ecotoxicol. Environ. Saf.* 95, 212–220. <https://doi.org/10.1016/j.ecoenv.2013.05.007>.
- Brazilian National Standards Organization, 2005. ABNT NBR ISO/IEC 17025: General Requirements for the Competence of Testing and Calibration Laboratories. ABNT, Rio de Janeiro.
- Brus, D.J., Lame, F.P.J., Nieuwenhuis, R.H., 2009. National baseline survey of soil quality in The Netherlands. *Environ. Pollut.* 157, 2043–2052. <https://doi.org/10.1016/j.envpol.2009.02.028>.
- Bucher, B., Davidoff, B., Amacher, M.C., Hinz, C., Iskandar, I.K., Selim, H.M., 1989. Correlation of Freundlich K_d and n retention parameters with soils and elements. *Soil Sci.* 148, 370–379. <https://doi.org/10.1097/00010694-198911000-00008>.
- Camargo, O.A., Moniz, A.C., Jorge, J.A., Valadares, J.M.A.S., 2009. Métodos de Análise Química, Mineralógica e Física de Solos do Instituto Agronômico de Campinas. Instituto Agronômico de Campinas, Campinas. http://www.iac.sp.gov.br/produtoseservicos/analisedosolo/docs/Boletim_Tecnico_106_rev_atual_2009.pdf.
- Camargo, O.A., Rovers, H., Valadares, J.M.A.S., 1989. Adsorção de níquel em Latossolos paulistas. *Rev. Bras. Cienc. Solo* 13, 125–129.
- Canteras, F.B., Oliveira, B.F.F., Moreira, S., 2019. Topsoil pollution in highway medians in the State of São Paulo (Brazil): determination of potentially toxic elements using synchrotron radiation total reflection X-ray fluorescence. *Environ. Sci. Pollut. Res.* Int. 26, 20839–20852. <https://doi.org/10.1007/s11356-019-05425-2>.
- Caritat, P., Reimann, C., Smith, D.B., Wang, X., 2018. Chemical elements in the environment: multi-element geochemical datasets from continental- to national-scale surveys on four continents. *Appl. Geochem.* 89, 150–159. <https://doi.org/10.1016/j.apgeochem.2017.11.010>.
- Carlton, C., Dalla Valle, M., Marcomini, A., 2004. Regression models to predict water-soil heavy metals partition coefficients in risk assessment studies. *Environ. Pollut.* 127, 109–115. [https://doi.org/10.1016/S0269-7491\(03\)00253-7](https://doi.org/10.1016/S0269-7491(03)00253-7).
- Casagrande, J.C., Soares, M.R., Mouta, E.R., 2008. Zinc adsorption in highly weathered soils. *Pesqui. Agropecu. Bras.* 43, 131–139. <https://doi.org/10.1590/S0100-204X2008000100017>.
- CETESB - Environmental Agency of the State of São Paulo, 2001. Report for establishment of guiding values for soils and groundwater of the State of São Paulo. <https://cetesb.sp.gov.br/solo/publicacoes-e-relatorios/>. (Accessed 22 August 2020).
- CETESB - Environmental Agency of the State of São Paulo, 2016. Valores orientadores para solos e águas subterrâneas no Estado de São Paulo 2016 (accessed 08 November 2020). https://cetesb.sp.gov.br/aguas-subterraneas/wp-content/uploads/sites/13/2013/11/tabelas_vos_2016_site.pdf.
- CETESB - Environmental Agency of the State of São Paulo, 2017. Decisão de Diretoria nº 038/2017/C, de 07 de fevereiro de 2017. <https://cetesb.sp.gov.br/wp-content/uploads/2014/12/DD-038-2017-C.pdf>. (Accessed 12 June 2020).
- CETESB - Environmental Agency of the State of São Paulo, 2019. Explanatory text: relationship of contaminated and rehabilitated areas in the State of São Paulo. Brazil. <https://cetesb.sp.gov.br/areas-contaminadas/wp-content/uploads/sites/17/2020/02/TEXTO-EXPLICATIVO-2019-12.02.20.pdf>. (Accessed 12 August 2020).
- CETESB - Environmental Agency of the State of São Paulo, 2020. Worksheets for risk assessment in contaminated areas under investigation. <https://cetesb.sp.gov.br/areas-contaminadas/planilhas-para-avaliacao/>. (Accessed 18 December 2020).
- Chang, C.M., Wang, M.K., Chang, T.W., Lin, C., Chen, Y.R., 2001. Transport modelling of copper and cadmium with linear and nonlinear retardation factor. *Chemosphere* 43, 1133–1139. [https://doi.org/10.1016/s0045-6535\(00\)00176-4](https://doi.org/10.1016/s0045-6535(00)00176-4).
- Chen, W., Li, L., Chang, A.C., Wu, L., Chaney, R.L., Smith, R., Ajwa, H., 2009. Characterizing the solid-solution partitioning coefficient and plant uptake factor of As, Cd, and Pb in California croplands. *Agric. Ecosyst. Environ.* 129, 212–220. <https://doi.org/10.1016/j.agee.2008.09.001>.
- CONAMA - Brazilian National Environment Council, 2009. Resolução nº 420, de 28 de dezembro de 2009. <http://www2.mma.gov.br/port/conama/legiabre.cfm?codigiequals;620>. (Accessed 10 June 2020).
- Covelo, E.F., Vega, F.A., Andrade, M.L., 2007. Simultaneous sorption and desorption of Cd, Cr, Ni, Cu, Pb and Zn in acid soils. I. Selectivity sequences. *J. Hazard Mater.* 147, 852–861. <https://doi.org/10.1016/j.jhazmat.2007.01.123>.
- Crommentijn, T., Polder, M.D., Van de Plassche, E.J., 1997. Maximum permissible concentrations and negligible concentrations for metals, taking background concentrations into account (RIVM Report nº 601501001). <http://www.rivm.nl/bibliotheek/rapporten/601501001.html>. (Accessed 24 November 2020).
- Cunha, R.C.A., Camargo, A.O., Kinjo, T., 1994. Aplicação de três isotermas na adsorção de zinco em Oxisolos, Alfissolos e Ultissolos. *Rev. Bras. Cienc. Solo* 18, 15–18.
- DAEE - Departamento de Águas e Energia Elétrica/LEBAC - Laboratório de Estudo de Bacias, 2013. Águas Subterrâneas no Estado de São Paulo: Diretrizes de Utilização e Proteção, DAEE/LEBAC, São Paulo. [http://201.55.6.68/acervoepesquisa/Atlas%20-20%C3%82%01guas%20Subterr%C3%A2neas%20\(DAEE-LEBAC\).pdf](http://201.55.6.68/acervoepesquisa/Atlas%20-20%C3%82%01guas%20Subterr%C3%A2neas%20(DAEE-LEBAC).pdf).
- Dane, J.H., Topp, C.G., 2002. Methods of Soil Analysis: Part 4-Physical Methods, Soil Science Society of America. Madison.
- Dreyse, F., Smolders, E., Parker, D.R., 2009. Partitioning of metals (Cd, Co, Cu, Ni, Pb, Zn) in soils: concepts, methodologies, prediction and applications - a review. *Eur. J. Soil Sci.* 60, 590–612. <https://doi.org/10.1111/j.1365-2389.2009.01142.x>.
- EMBRAPA - Brazilian Agricultural Research Corporation, 2017. Manual de Métodos de Análise de Solo, third ed. EMBRAPA, Brasília DF <https://www.infoteca.cnptia.embrapa.br/handle/doc/1085209>.
- EMBRAPA - Brazilian Agricultural Research Corporation, 2018. Brazilian Soil Classification System, fifth ed. EMBRAPA, Brasília DF <https://www.embrapa.br/en/solos/sibcs>.
- Environmental Agency, 2005. Development of the partition coefficient (K_d) test method for use in environmental risk assessments (Science Report SC020039/4). https://assets.publishing.service.gov.uk/government/uploads/system/uploads/attachment_data/file/290425/scho0705bjz-e-e.pdf. (Accessed 5 September 2020).
- Fabiatti, G., Biasioli, M., Barberis, R., Ajmone-Marsan, F., 2009. Soil contamination by organic and inorganic pollutants at the regional scale: the case of Piedmont, Italy. *J. Soil Sedim.* 10, 290–300. <https://doi.org/10.1007/s11368-009-0114-9>.
- Fendorf, S.E., 1995. Surface reactions of chromium in soils and waters. *Geoderma* 67, 55–71. [https://doi.org/10.1016/0016-7061\(94\)00062-F](https://doi.org/10.1016/0016-7061(94)00062-F).
- Fernandes, A., Santos, E.S., Braz, A.M.S., Birani, S.M., Alleoni, L.R.F., 2018. Quality reference values and background concentrations of potentially toxic elements in soils from the Eastern Amazon. Brazil. *J. Geochem. Explor.* 190, 453–463. <https://doi.org/10.1016/j.gexplo.2018.04.012>.
- Fontes, M.P.F., Alleoni, L.R.F., 2006. Electrochemical attributes and availability of nutrients, toxic elements, and heavy metals in tropical soils. *Sci. Agric.* 63, 589–608. <https://doi.org/10.1590/S0103-90162006000600014>.
- Galán, E., Romero-Baena, A.J., Aparicio, P., González, I., 2019. A methodological approach for the evaluation of soil pollution by potentially toxic trace elements. *J. Geochem. Explor.* 203, 96–107. <https://doi.org/10.1016/j.gexplo.2019.04.005>.

- Gerritse, R.G., Van Driel, W., 1984. The relationship between adsorption of trace metals, organic matter, and pH in temperate soils. *J. Environ. Qual.* 13, 197–204. <https://doi.org/10.2134/jeq1984.00472425001300020005x>.
- Gil-García, C., Tagami, K., Uchida, S., Rigol, A., Vidal, M., 2009. New best estimates for radionuclide solid–liquid distribution coefficients in soils. Part 3: miscellany of radionuclides (Cd, Co, Ni, Zn, I, Se, Sb, Pu, Am, and others). *J. Environ. Radioact.* 100, 704–715. <https://doi.org/10.1016/j.jenvrad.2008.12.001>.
- Gmach, M.R., Cherubin, M.R., Kaiser, K., Cerri, C.E.P., 2019. Processes that influence dissolved organic matter in the soil: a review. *Sci. Agric.* 77, 1–10. <https://doi.org/10.1590/1678-992x-2018-0164>.
- Gomes, P.C., Fontes, M.P.F., Silva, A.G., Mendonça, E.S., Netto, A.R., 2001. Selectivity sequence and competitive adsorption of heavy metals by Brazilian soils. *Soil Sci. Soc. Am. J.* 65, 1115–1121. <https://doi.org/10.2136/sssaj2001.6541115x>.
- González-Costa, J.J., Reigosa, M.J., Matías, J.M., Fernández-Covelo, E., 2017. Analysis of the importance of oxides and clays in Cd, Cr, Cu, Ni, Pb and Zn adsorption and retention with regression trees. *PLoS One* 12, 1–25. <https://doi.org/10.1371/journal.pone.0168523>.
- Harter, R.D., Naidu, R., 2001. An assessment of environmental and solution parameter impact on trace-metal sorption by soils. *Soil Sci. Soc. Am. J.* 65, 597–612. <https://doi.org/10.2136/sssaj2001.653597x>.
- Harter, R.D., 1983. Effect of soil pH on adsorption of lead, copper, zinc, and nickel. *Soil Sci. Soc. Am. J.* 47, 47–51. <https://doi.org/10.2136/sssaj1983.03615995004700010009x>.
- Hinz, C., 2001. Description of sorption data with isotherm equations. *Geoderma* 99, 225–243. [https://doi.org/10.1016/S0016-7061\(00\)00071-9](https://doi.org/10.1016/S0016-7061(00)00071-9).
- Holm, P.E., Rootzén, H., Borggaard, O.K., Moberg, J.P., Christensen, T.H., 2003. Correlation of cadmium distribution coefficients to soil characteristics. *J. Environ. Qual.* 32, 138–145. <https://doi.org/10.2134/jeq2003.0138>.
- Houba, V.J.G., Lexmond, T.M., Novozamsky, I., van der Lee, J.J., 1996. State of the art and future developments in soil analysis for bioavailability assessment. *Sci. Total Environ.* 1–3, 21–28. [https://doi.org/10.1016/0048-9697\(95\)04793-X](https://doi.org/10.1016/0048-9697(95)04793-X).
- IBGE - Brazilian Institute of Geography and Statistics, 2019. Produto Interno Bruto dos Municípios 2017. IBGE, Rio de Janeiro. <https://biblioteca.ibge.gov.br/visualizacao/livros/liv101688/informativo.pdf>.
- ISO - International Standard Organization, 2012. ISO 12914: Soil Quality - Microwave-Assisted Extraction of the Aqua Regia Soluble Fraction for the Determination of Elements, first ed. ISO, Geneva.
- Janssen, R.P.T., Peijnenburg, W.J.G.M., Posthuma, L., Hoop, M.A.G.T., 1997. Equilibrium partitioning of heavy metals in Dutch Field soils. I. Relationship between metal partition coefficients and soil characteristics. *Environ. Toxicol. Chem.* 16, 2470–2478. <https://doi.org/10.1002/etc.5620161206>.
- Jardine, P.M., Weber, N.L., McCarthy, J.F., 1989. Mechanisms of dissolved organic carbon adsorption on soil. *Soil Sci. Soc. Am. J.* 53, 1378–1385. <https://doi.org/10.2136/sssaj1989.03615995005300050013x>.
- Jeffries, J., Martin, I., 2009. Updated technical background to the CLEA model (Science Report SC050021/SR3). <https://www.gov.uk/government/publications/updated-technical-background-to-the-clea-model>. (Accessed 19 May 2020).
- Jennings, A.A., 2013. Analysis of worldwide regulatory guidance values for the most commonly regulated elemental surface soil contamination. *J. Environ. Manag.* 118, 72–95. <https://doi.org/10.1016/j.jenvman.2012.12.032>.
- Kaiser, K., Guggenberger, G., 2003. Mineral surfaces and soil organic matter. *Eur. J. Soil Sci.* 54, 219–236. <https://doi.org/10.1046/j.1365-2389.2003.00544.x>.
- Kalbasi, M., Racz, G.J., Loewen-Rudgers, L.A., 1978. Mechanism of zinc adsorption by iron and aluminum oxides. *Soil Sci.* 125, 146–150.
- Kämpf, N., Curi, N., Marques, J., 2019. Intemperismo e ocorrência de minerais no ambiente do solo. In: Melo, V.F., Alleoni, L.R.F. (Eds.), *Química e Mineralogia do Solo: ociedade Brasileira de Ciéncia do Solo, Viçosa*, pp. 333–380.
- Kim, R.Y., Yoon, J.K., Kim, T.S., Yang, J.E., Owens, G., Kim, K.R., 2015. Bioavailability of heavy metals in soils: definitions and practical implementation - a critical review. *Environ. Geochem. Health* 36, 1041–1061. <https://doi.org/10.1007/s10653-015-9695-y>.
- Koning, A., Geelhoed-Bonouvre, P.A., Comans, R.N.J., 2000. Comparing in situ distribution coefficients and exchangeability of radiocesium in freshwater sediments with laboratory predictions. *Sci. Total Environ.* 120, 29–35. [https://doi.org/10.1016/S0048-9697\(00\)00495-2](https://doi.org/10.1016/S0048-9697(00)00495-2).
- Lee, S.W., Cho, H.G., Kim, S.O., 2019. Comparisons of human risk assessment models for heavy metal contamination within abandoned metal mine areas in Korea. *Environ. Geochem. Health* 41, 481–505. <https://doi.org/10.1007/s10653-018-0108-x>.
- Lee, S.Z., Allen, H.E., Huang, C.P., Sparks, D.L., Sanders, P.F., Peijnenburg, W.J.G.M., 1996. Predicting soil-water partition coefficients for cadmium. *Environ. Sci. Technol.* 30, 3418–3424. <https://doi.org/10.1021/es9507933>.
- Limousin, G., Gaudet, J.P., Charlet, L., Szenknect, S., Barthès, V., Krimissa, M., 2007. Sorption isotherms: a review on physical bases, modeling and measurement. *Appl. Geochem.* 22, 249–275. <https://doi.org/10.1016/j.apgeochem.2006.09.010>.
- Linhares, L.A., Egreja Filho, F.B., Oliveira, C.V., Bellis, V., 2009. Adsorção de cádmio e chumbo em solos tropicais altamente intemperizados. *Pesqui. Agropecu. Bras.* 44, 291–299. <https://doi.org/10.1590/S0100-204X2009000300011>.
- Liu, I., Li, W., Song, W., Guo, M., 2018. Remediation techniques for heavy metal-contaminated soils: principles and applicability. *Sci. Total Environ.* 633, 206–219. <https://doi.org/10.1016/j.scitotenv.2018.03.161>.
- Matos, A.T., Fontes, M.P.F., Costa, L.M., Martinez, M.A., 2001. Mobility of heavy metals as related to soil chemical and mineralogical characteristics of Brazilian soils. *Environ. Pollut.* 111, 429–435. [https://doi.org/10.1016/S0269-7491\(00\)00088-9](https://doi.org/10.1016/S0269-7491(00)00088-9).
- Matos, A.T., Fontes, M.P.F., Jordão, C.P., Costa, L.M., 1996. Mobilidade e formas de metais pesados em Latossolo Vermelho-Amarelo. *Rev. Bras. Cienc. Solo* 20, 379–386. <https://doi.org/10.1590/S0103-90162001000400024>.
- Matusiewicz, H., Bulska, E., 2018. *Inorganic Trace Analytics - Trace Elements Analysis and Speciation*, first ed. De Gruyter, Berlin.
- McBride, M.B., 1989. Reactions controlling heavy metal solubility in soils. *Adv. Soil Sci.* 10, 1–56. https://doi.org/10.1007/978-1-4613-8847-0_1.
- Millard, S.P., 2019. EPA is mandating the normal distribution. *Stat. Publ. Pol.* 6, 36–43. <https://doi.org/10.1080/2330443X.2018.1564639>.
- Mouta, E.R., Soares, M.R., Casagrande, J.C., 2008. Copper adsorption as a function of solutions parameters of variable charge soils. *J. Braz. Chem. Soc.* 19, 996–1009. <https://doi.org/10.1590/S0103-50532008000500027>.
- Müller, T., Höper, H., 2004. Soil organic matter turnover as a function of the soil clay content: consequences for model applications. *Soil Biol. Biochem.* 36, 877–888. <https://doi.org/10.1016/j.soilbio.2003.12.015>.
- Nogueira, T.A.R., Abreu-Júnior, C.H., Alleoni, L.R.F., He, Z., Soares, M.R., Vieira, C.S., Lessa, L.G.F., Capra, F., 2018. Background concentrations and quality reference values for some potentially toxic elements in soils of São Paulo State. *Brazil. J. Environ. Manag.* 221, 10–19. <https://doi.org/10.1016/j.jenvman.2018.05.048>.
- Otte, P.F., Lijzen, J.P.A., Otte, J.G., Swartjes, F.A., Verslujs, C.W., 2001. Evaluation and revision of the CSOL parameters set: proposed parameter set for human exposure modelling and deriving intervention values for the first series of compounds (RIVM Report n° 711701021). <https://www.rivm.nl/bibliotheek/rapporten/711701021.html>. (Accessed 10 July 2020).
- Palanosooriya, K.N., Shaheen, S.M., Chen, S.S., Tsang, D.C.W., Hashimoto, Y., Hou, D., Bolan, N.S., Rinklebe, J., Ok, Y.S., 2020. Soil amendments for immobilization of potentially toxic elements in contaminated soils: a critical review. *Environ. Int.* 134, 1–29. <https://doi.org/10.1016/j.envint.2019.105046>.
- Panagos, P., Liedekerke, M.V., Yigini, Y., Montanarella, L., 2013. Contaminated sites in Europe: review of the current situation based on data collected through a European network. *J. Environ. Public Health* 13, 1–11. <https://doi.org/10.1155/2013/158764>.
- Paye, H., Mello, J.W.V., Abrahão, W.A.P., Fernandes Filho, E.I., Dias, L.C.P., Castro, M.L.O., Melo, S.B., França, M.M., 2010. Reference quality values for heavy metals in soils from Espírito Santo state. *Rev. Bras. Cienc. Solo* 36, 1031–1042. <https://doi.org/10.1590/S0100-0683201000600028>.
- Peng, S., Wang, P., Peng, L., Cheng, T., Sun, W., Shi, Z., 2018. Predicting heavy metal partition equilibrium in soils: roles of soil components and binding sites. *Soil Sci. Soc. Am. J.* 82, 839–849. <https://doi.org/10.2136/sssaj2018.03.0104>.
- Pérez, A.P., Eugenio, N.R., 2018. Status of Local Soil Contamination in Europe: Revision of the Indicator "Progress in the Management Contaminated Sites in Europe" (JCR Technical Reports EUR 29124-EN). Publications Office of the European Union, Luxembourg. <https://doi.org/10.2760/093804>.
- Pettenati, M., Surdyk, N., Cary, L., Kloppmann, W., 2016. Revisiting the K_f distribution coefficient concept through stringent geochemical modeling: application to agronomical models under wastewater reclamation context. *Geoderma* 268, 128–138. <https://doi.org/10.1016/j.geoderma.2016.01.020>.
- Qu, C., Chen, W., Hu, X., Cai, P., Chen, C., Yu, X.Y., Huang, Q., 2019. Heavy metal behavior at mineral-organo interfaces: mechanisms, modelling and influence factors. *Environ. Int.* 131, 1–15. <https://doi.org/10.1016/j.envint.2019.104995>.
- R CORE TEAM, 2017. R: A Language and Environment for Statistical Computing. Vienna. <http://www.R-project.org>.
- Rai, P.K., Lee, S.S., Zhang, M., Tsang, Y.F., Kim, K.H., 2019. Heavy metals in food crops: health risks, fate, mechanisms, and management. *Environ. Int.* 125, 365–385. <https://doi.org/10.1016/j.envint.2019.01.067>.
- Raij, B., van Andrade, J.C., Cantarella, H., Quaggio, J.A., 2001. Análise Química para Avaliação da Fertilidade de Solos Tropicais, IAC - Instituto Agronômico de Campinas. Campinas.
- Rasmussen, C., Heckman, K., Wieder, W.R., Keiliweit, M., Lawrence, C.R., Berhe, A.A., Blankinship, J.C., Crow, S.E., Druhan, J.L., Pries, C.E.H., Marin-Spiotta, E., Plante, A.F., Schädle, C., Schimel, J.P., Sierra, C.A., Wagai, R., 2018. Beyond clay: towards an improved set of variables for predicting soil organic matter content. *Biogeochemistry* 137, 297–306. <https://doi.org/10.1007/s10533-018-0424-3>.
- Rieuwerts, J.S., 2007. The mobility and bioavailability of trace metals in tropical soils: a review. *Chem. Speciat. Bioavailab.* 19, 75–85. <https://doi.org/10.3184/095422907X211918>.
- Robbins, J.L., Daneman, J.C., 1999. Parametric estimating and stepwise statistical technique. *National Estimator* 4, 24–34.
- Rodrigues, S.M., Pereira, M.E., Ferreira da Silva, E., Hursthorne, A.S., Duarte, A.C., 2009. A review of regulatory decisions for environmental protection: Part I - challenges in the implementation of national soil policies. *Environ. Int.* 35, 202–213. <https://doi.org/10.1016/j.envint.2008.08.007>.
- Rodushkin, I., Engström, E., Baxter, D.C., 2010. Sources of contamination and remedial strategies in the multi-elemental trace analysis laboratory. *Anal. Bioanal. Chem.* 396, 365–377. <https://doi.org/10.1007/s00216-009-3087-z>.
- Rossi, M., 2017. Mapa Pedológico do Estado de São Paulo: Revisado e Ampliado, Secretaria do Meio Ambiente/Instituto Florestal, São Paulo. <https://www.infr>

- aestruturameioambiente.sp.gov.br/institutoforestal/wp-content/uploads/sites/234/2017/11/Livro_Solos1.pdf.
- Sakamoto, Y., Ishiguro, M., Kitagawa, G., 1986. Akaike Information Criterion Statistics. Reidel, Dordrecht.
- Santos, S.N., Alleoni, L.R.F., 2012. Reference values for heavy metals in soils of Brazilian agricultural frontier in Southwestern Amazonia. Environ. Monit. Assess. 185, 5737–5748. <https://doi.org/10.1007/s10661-012-2980-7>.
- SÃO PAULO, 2009. Lei nº 13.577, de 8 de julho de 2009. <https://www.al.sp.gov.br/repositorio/legislacao/lei/2009/lei-13577-08.07.2009.html>. (Accessed 20 September 2020).
- Sauvé, S., Hendershot, W., Allen, H.E., 2000. Solid-solution partitioning of metals in contaminated soils: dependence on pH, total metal burden, and organic matter. Environ. Sci. Technol. 34, 1125–1131. <https://doi.org/10.1021/es9907764>.
- Schaefer, C.E.G.R., Fabris, J.D., Ker, J.C., 2008. Minerals in the clay fraction of Brazilian Latosols (Oxisols): a review. Clay Miner. 43, 137–154. <https://doi.org/10.1180/claymin.2008.043.1.11>.
- Schneider, A., Nguyen, V.X., Viala, Y., Violo, V., Cornu, J.Y., Thibault, T., Nguyen, C., 2019. A method to determine the soil-solution distribution coefficients and the concentrations for the free ion and the complexes of trace metals: application to cadmium. Geoderma 346, 91–102. <https://doi.org/10.1016/j.geoderma.2019.02.001>.
- Shaheen, S.M., Tsadilas, C.D., Rinklebe, J., 2013. A review of the distribution coefficients of trace elements in soils: influence of sorption system, element characteristics, and soil colloidal properties. Adv. Colloid Interface Sci. 201–202, 43–56. <https://doi.org/10.1016/j.cis.2013.10.005>.
- Sheppard, M.I., Sheppard, S.C., Grant, C.A., 2007. Solid/liquid partition coefficients to model trace element critical loads for agricultural soils in Canada. Can. J. Soil Sci. 87, 189–201. <https://doi.org/10.4141/S06-061>.
- Sheppard, M.I., Thibault, D.H., 1990. Default soil solid liquid partition-coefficients, K_d , for four major soil types - a compendium. Health Phys. 59, 471–482. PMID:2398015.
- Sheppard, S.C., 2011. Robust prediction of K_d from soil properties for environmental assessment. Hum. Ecol. Risk Assess. 17, 263–279. <https://doi.org/10.1080/10807039.2011.538641>.
- Shi, Z., Peng, S., Lin, X., Liang, Y., Lee, S.Z., Allen, H.E., 2020. Predicting Cr(VI) adsorption on soils: the role of the competition of soil organic matter. Environ. Sci. Proc. Imp. 22, 95–104. <https://doi.org/10.1039/C9EM00477G>.
- SIFESP – São Paulo State Forestry Information System, 2010. Inventário florestal da vegetação natural do Estado de São Paulo. <https://www.infraestruturameioambiente.sp.gov.br/sifesp/tabelas-pdf/>. (Accessed 2 August 2020).
- Silveira, M.L.A., Alleoni, L.R.F., Casagrande, J.C., Camargo, O.A., 2002. Copper adsorption in oxidic soils after removal of organic matter and iron oxide. Commun. Soil Sci. Plant Anal. 33, 3581–3592. <https://doi.org/10.1081/CSS-120015907>.
- Silveira, M.L.A., Alleoni, L.R.F., 2003. Copper adsorption in tropical Oxisols. Braz. Arch. Biol. Technol. 46, 529–536. <https://doi.org/10.1590/S1516-89132003000400006>.
- Six, J., Feller, C., Denef, K., Ogle, S.M., Sá, J.C.M., Albrecht, A., 2002. Soil organic matter, biota and aggregation in temperate and tropical soils - effects of no-tillage. Agronomie 22, 755–775. <https://doi.org/10.1051/agro:2002043>.
- Smith, D.B., Smith, S.M., Horton, J.D., 2013. History and evaluation of national-scale geochemical data sets for the United States. Geosci. Front. 4, 167–183. <https://doi.org/10.1016/j.gsf.2012.07.002>.
- Soares, M.R., Alleoni, L.R.F., 2008. Contribution of soil organic carbon to the ion exchange capacity of tropical soils. J. Sustain. Agric. 32, 439–462. <https://doi.org/10.1080/10440040802257348>.
- Soares, M.R., Casagrande, J.C., Mouta, E.R., 2009. Effects of soil solution parameters on cadmium adsorption by Brazilian variable charge soils. Commun. Soil Sci. Plant Anal. 32, 2132–2151. <https://doi.org/10.1080/00103620902960633>.
- Soares, M.R., Casagrande, J.C., Mouta, E.R., 2011. Nickel adsorption by variable charge soils: effect of pH and ionic strength. Braz. Arch. Biol. Technol. 54, 207–220. <https://doi.org/10.1590/S1516-89132011000100025>.
- Soares, M.R., Casagrande, J.C., 2009. Adsorção e modelos. In: Ribeiro, M.R., Nascimento, C.W.A., Cantalice, J.R.B., Ribeiro Filho, M.R. (Eds.), Tópicos em Ciência do Solo. Sociedade Brasileira de Ciência do Solo, Viçosa, pp. 71–201.
- Soares, M.R., 2004. Distribution Coefficient (K_d) of Heavy Metals in Soils of the State of São Paulo. University of São Paulo. PhD Thesis. <https://www.teses.usp.br/teses/diponiveis/11/11140/tde-31052005-170719/publico/marcio.pdf>.
- Soil Survey Staff, 2014. Keys to Soil Taxonomy, Twelfth Ed. USDA-Natural Resources Conservation Service. Washington DC. https://www.nrcs.usda.gov/wps/portal/nrcs/detail/soils/survey/class/?cid=&quals;nrcs142p2_053580.
- Souza, J.J.L.L., Abrahão, W.A.P., Mello, J.W.V., Silva, J., Oliveira, T.S., 2015. Geochemistry and spatial variability of metal(lloid) concentrations in soils of the state of Minas Gerais. Brazil. Sci. Total Environ. 505, 338–349. <https://doi.org/10.1016/j.scitotenv.2014.09.098>.
- Spark, K.M., Johnson, B.B., Wells, J.D., 1995. Characterizing heavy-metal adsorption on oxides and oxyhydroxides. Eur. J. Soil Sci. 46, 621–631. <https://doi.org/10.1111/j.1365-2389.1995.tb01358.x>.
- Sparks, D.L., Page, A.L., Helmke, P.A., Loepert, R.H., 1996. Methods of Soil Analysis: Part 3-Chemical Methods, Soil Science Society of America. Madison.
- Spínola, A.L.S., Philippi Jr., A., 2011. Contaminated sites and public policies in São Paulo State, Brazil. In: Broniewicz, E. (Ed.), Environmental Management in Practice. InTech, Rijeka, pp. 145–158.
- Sposito, G., 1989. The Chemistry of Soils. Oxford, New York.
- StatSoft Inc, 2014. Statistica: data analysis software system. Version 10.0. www.statsoft.com. (Accessed 14 February 2020).
- Stevenson, F.J., 1994. Humus Chemistry: Genesis, Composition, and Reactions, second ed. John Wiley, New York.
- Sun, R., Chen, L., 2016. Assessment of heavy metal pollution in topsoil around Beijing Metropolis. PloS One 11, 1–13. <https://doi.org/10.1371/journal.pone.0155350>.
- Swartjes, F.A., Rutgers, M., Lijzen, J.P.A., Janssen, P.J.C.M., Otte, P.F., Wintersen, A., Brand, E., Posthuma, L., 2012. State of the art of contaminated site management in The Netherlands: policy framework and risk assessment tools. Sci. Total Environ. 427–428, 1–10. <https://doi.org/10.1016/j.scitotenv.2012.02.078>.
- Takata, H., Tagami, K., Aono, T., Uchida, S., 2014. Distribution coefficients (K_d) of strontium and significance of oxides and organic matter in controlling its partitioning in coastal regions of Japan. Sci. Total Environ. 490, 979–986. <https://doi.org/10.1016/j.scitotenv.2014.05.101>.
- Temminghoff, E.J.M., Van der Zee, S.E.A.T.M., Haan, F.A.M., 1997. Copper mobility in a copper-contaminated sandy soil as affected by pH and solid and dissolved organic matter. Environ. Sci. Technol. 31, 1109–1115. <https://doi.org/10.1021/es9606236>.
- Tipping, E., Rieuwerts, J., Pan, G., Ashmore, M.R., Loftis, S., Hill, M.T.R., Farago, M.E., Thornton, I., 2003. The solid-solution partitioning of heavy metals (Cu, Zn, Cd, Pb) in upland soils of England and Wales. Environ. Pollut. 125, 213–225. [https://doi.org/10.1016/S0269-7491\(03\)00058-7](https://doi.org/10.1016/S0269-7491(03)00058-7).
- Tukey, J.W., 1977. Exploratory Data Analysis: Box-And-Whisker Plots. Addison-Wesley, Reading.
- Ulery, A.L., Drees, L.R., 2008. Methods of Soil Analysis: Part 5-Mineralogical Methods, Soil Science Society of America, Madison.
- USEPA - United States Environmental Protection Agency, 1989. Risk assessment guidance for Superfund - human health evaluation manual (Part A) (EPA/540/1-89/002). https://www.epa.gov/sites/production/files/2015-09/documents/rags_a.pdf. (Accessed 14 September 2020).
- USEPA - United States Environmental Protection Agency, 1996. Soil screening guidance: technical background document (EPA/540/R95/128). <https://www.epa.gov/superfund/superfund-soil-screening-guidance>. (Accessed 14 September 2020).
- USEPA - United States Environmental Protection Agency, 1999. Understanding variation in partition coefficient, K_d , values - the K_d model, methods of measurement, and application of chemical reaction codes (EPA 402-R-99-9004A). <https://www.epa.gov/sites/production/files/2015-05/documents/402-r-99-004a.pdf>. (Accessed 15 September 2020).
- USEPA - United States Environmental Protection Agency, 2008. Fate, transport and transformation test guidelines - OPPTS 835.1230 Adsorption/Desorption (Batch Equilibrium) (EPA 712-C-08-009). <https://www.regulations.gov/document?D=&quals;EPA-HQ-OPPT-2009-0152-0006>. (Accessed 20 September 2020).
- USEPA - United States Environmental Protection Agency, 2014. Cleaning up the Nation's Waste Sites: Markets and Technology Trends (EPA 542-R-04-015), 2014 ed. Office of Solid Waste and Emergency Response, Washington DC. <https://nepis.epa.gov/EEx/ZyPDF.cgi/30006II3.PDF?Dockey=&quals;30006II3.PDF>
- USEPA - United States Environmental Protection Agency, 2015a. Priority pollutant list (40 CFR Part 423, Appendix A). <https://www.epa.gov/sites/production/files/2015-09/documents/priority-pollutant-list-epa.pdf>. (Accessed 13 December 2020).
- USEPA - United States Environmental Protection Agency, 2015b. ProUCL version 5.1 technical guide - statistical software for environmental applications for data sets with and without nondetect observations (EPA/600/R-07/041). https://www.epa.gov/sites/production/files/2016-05/documents/proucl_5.1_tech-guide.pdf. (Accessed 13 December 2020).
- USEPA - United States Environmental Protection Agency, 2015c. The SW-846 compendium: 3000 series – inorganic sample preparation. <https://www.epa.gov/hw-sw846/sw-846-compendium>. (Accessed 7 October 2020).
- USEPA - United States Environmental Protection Agency, 2018. Superfund task force recommendations 2018 updates. <https://semspub.epa.gov/work/HQ/197209.pdf>. (Accessed 10 December 2020).
- USEPA - United States Environmental Protection Agency, 2019. Regional screening levels (RSLS) - generic tables. <https://www.epa.gov/risk/regional-screening-levels-rsls-generic-tables>. (Accessed 8 December 2020).
- USEPA - United States Environmental Protection Agency, 2020. EPA's IRIS program - integrated risk information system. <https://www.epa.gov/iris>. (Accessed 13 December 2020).
- Vitale, C.M., Di Guardo, A., 2019. A review of the predictive models estimating association of neutral and ionizable organic chemicals with dissolved organic carbon. Sci. Total Environ. 666, 1022–1032. <https://doi.org/10.1016/j.scitotenv.2019.02.340>.
- VROM - Ministry of Housing, Spatial Planning and Environment, 1994. Intervention Values and Target Values: Soil Quality Standards (DBO/07494013). VROM, The Hague.
- Wiatrowska, K., Komisarek, J., 2019. Role of the light fraction of soil organic matter in trace elements binding. PloS One 14, 1–15. <https://doi.org/10.1371/journal.pone.0217077>.
- Wiseman, C.L.S., Püttman, W. Interactions between mineral phases in the preservation of soil organic matter. Geoderma 134, 109–118. <https://doi.org/10.1016/j.geoderma.2005.09.001>.

- Wuana, R.A., Okieme, F.E., 2011. Heavy metals in contaminated soils: a review of sources, chemistry, risks and best available strategies for remediation. *Int. Scholarly Res. Notices*, 1–20. <https://doi.org/10.5402/2011/402647>.
- Yen Le, T.T., Hendricks, A.J., 2014. Uncertainties associated with lacking data for predictions of solid-solution partitioning of metals in soil. *Sci. Total Environ.* 490, 44–49. <https://doi.org/10.1016/j.scitotenv.2014.04.124>.
- Yin, Y., Impellitteri, C.A., You, S.J., Allen, H.E., 2002. The importance of organic matter distribution and extract soil:solution ratio on the desorption of heavy metals from soils. *Sci. Total Environ.* 287, 107–119. [https://doi.org/10.1016/S0048-9697\(01\)01000-2](https://doi.org/10.1016/S0048-9697(01)01000-2).
- Young, R., Mulligan, C.N., 2019. *Natural and Enhanced Attenuation of Contaminants in Soils*, second ed. CRC Press, Boca Raton.
- Yu, T.R., 1997. *Chemistry of Variable Charge Soils*. Oxford University Press, New York.
- Zhang, X., Li, J., Wei, D., Li, B., Ma, Y., 2018. The solid-solution distribution of copper added to soils: influencing factors and models. *J. Soils Sediments* 18, 2960–2969. <https://doi.org/10.1007/s11368-018-1962-y>.
- Zhang, Y.-Y., Wu, W., Li, H., 2019. Factors affecting variations of soil pH in different horizons in hilly regions. *PLoS One* 14, 1–13. <https://doi.org/10.1371/journal.pone.0218563>.